



Universiteit  
Leiden  
The Netherlands

## **The road to Insurmountability: Novel avenues to better target CC Chemokine Receptors**

Ortiz Zacarías, N.V.

### **Citation**

Ortiz Zacarías, N. V. (2019, December 4). *The road to Insurmountability: Novel avenues to better target CC Chemokine Receptors*. Retrieved from <https://hdl.handle.net/1887/81379>

Version: Publisher's Version

License: [Licence agreement concerning inclusion of doctoral thesis in the Institutional Repository of the University of Leiden](#)

Downloaded from: <https://hdl.handle.net/1887/81379>

**Note:** To cite this publication please use the final published version (if applicable).

Cover Page



Universiteit Leiden



The handle <http://hdl.handle.net/1887/81379> holds various files of this Leiden University dissertation.

**Author:** Ortiz Zacarías, N.V.

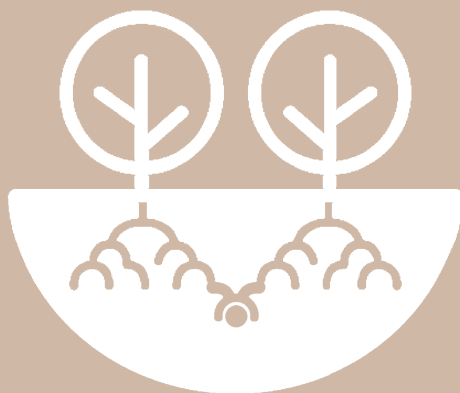
**Title:** The road to Insurmountability: Novel avenues to better target CC Chemokine Receptors

**Issue Date:** 2019-12-04

## Chapter 4

---

# Pyrrolone derivatives as intracellular allosteric modulators for chemokine receptors: Selective and dual-targeting inhibitors of CC Chemokine Receptors 1 and 2



*Natalia V. Ortiz Zacarías, Jacobus P.D. van Veldhoven, Laura Portner, Eric van Spronsen, Salviana Ullo, Margo Veenhuizen, Wijnand J.C. van der Velden, Annelien J.M. Zweemer, Roy M. Kreekel, Kenny Oenema, Eelke B. Lenselink, Laura H. Heitman, and Adriaan P. IJzerman*

*Journal of Medicinal Chemistry* 2018, 61 (20): 9146-9161



## ABSTRACT

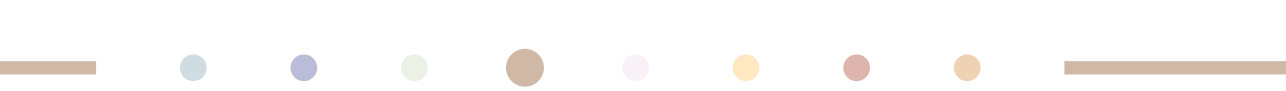
The recent crystal structures of CC chemokine receptors 2 and 9 (CCR2 and CCR9) have provided structural evidence for an allosteric, intracellular binding site. The high conservation of residues involved in this site suggests its presence in most chemokine receptors, including the close homolog CCR1. By using [<sup>3</sup>H]CCR2-RA-[R], a high-affinity, CCR2 intracellular ligand, we report an intracellular binding site in CCR1, where this radioligand also binds with high affinity. In addition, we report the synthesis and biological characterization of a series of pyrrolone derivatives for CCR1 and CCR2, which allowed us to identify several high-affinity intracellular ligands, including selective and potential multi-target antagonists. Evaluation of selected compounds in a functional [<sup>35</sup>S]GTPγS assay revealed that they act as inverse agonists in CCR1, providing a new manner of pharmacological modulation. Thus, this intracellular binding site enables the design of selective and multi-target inhibitors as a novel therapeutic approach.

## INTRODUCTION

Chemokines are chemotactic cytokines that control the migration and positioning of immune cells during physiological and pathological conditions by interacting with more than 20 different chemokine receptors.<sup>1</sup> Chemokine receptors mainly belong to the class A of G protein-coupled receptors (GPCRs), and can be divided into four different subtypes—namely C, CC, CXC and CX3C—according to the pattern of specific cysteine residues in their major endogenous chemokines.<sup>2</sup> To exert their function, chemokines bind at the extracellular side of their receptors in a binding mechanism involving the N-terminal domain, extracellular loops and the upper half of the transmembrane bundle.<sup>3,4</sup> After activation, most chemokine receptors signal through heterotrimeric G proteins, mainly G<sub>i/o</sub> class, and  $\beta$ -arrestins.<sup>2</sup> CC Chemokine receptors 1 (CCR1) and 2 (CCR2) are two of the ten members of the CC subtype of chemokine receptors. CCR1 and CCR2 are expressed in a variety of immune cells, such as monocytes, dendritic cells and T helper type-1 (T<sub>H</sub>1) cells, from where they regulate diverse inflammatory and homeostatic functions.<sup>5</sup> Multiple chemokines activate these two receptors, including CCL3, CCL5 and CCL8 in the case of CCR1; and CCL2, CCL7 and CCL8 in the case of CCR2.<sup>2</sup>

Dysregulation of CCR1, CCR2 and their ligands has been linked to several inflammatory and immune diseases,<sup>6,7</sup> which has resulted in many drug discovery efforts to develop small molecules that target these receptors.<sup>8,9</sup> Several lines of evidence support a role for both CCR1 and CCR2 in the pathogenesis of diseases such as rheumatoid arthritis (RA) and multiple sclerosis (MS): increased expression of both receptors and their ligands in disease models and patients;<sup>10,11</sup> protective effect of genetic knockout of CCR1 or CCR2 in disease models;<sup>12,13</sup> and positive preclinical studies with chemokine-neutralizing monoclonal antibodies or small-molecule inhibitors of CCR1 or CCR2.<sup>14-16</sup> Yet, only few clinical studies have shown promising results,<sup>17,18</sup> while most of the drugs developed so far have failed in clinical trials due to lack of efficacy.<sup>8,9</sup> In this regard, the development of multi-target drugs has been proposed as a strategy to overcome the lack of efficacy. Multi-target drugs are designed to specifically act on more than one drug target, which might be necessary in highly heterogeneous diseases, such as RA and MS, where more than one chemokine receptor is involved.<sup>19</sup> The design of dual-antagonists has been previously undertaken for CCR1/CCR3,<sup>20</sup> CCR2/CCR5,<sup>21</sup> CCR5/CXCR4,<sup>22</sup> and CXCR1/CXCR2;<sup>23</sup> however no CCR1/CCR2 dual-antagonists have so far been reported.

Recently, the crystal structures of CCR2 (**Chapter 3**)<sup>24</sup> and CCR9<sup>25</sup> have revealed a novel allosteric binding site for small molecules in chemokine receptors. Both CCR2-RA-[R] in CCR2 and vercirnon in CCR9 bind in a pocket located in the intracellular surface of the receptors, partially overlapping with the binding site for G proteins and  $\beta$ -arrestins (**Chapter**



3).<sup>24, 25</sup> These intracellular ligands can inhibit the receptors in a non-competitive and insurmountable manner with regard to chemokine binding, as demonstrated previously in CCR2.<sup>26</sup> This might result in higher efficacy even in the presence of a high local concentration of chemokines during a disease state. Together with the potential advantages of allosteric modulators of chemokine receptors, this intracellular binding site seems to be quite conserved among chemokine receptors, which suggests the presence of homologous pockets in other receptors such as CCR1 (**Chapter 2**).<sup>27</sup> This conservation might provide an opportunity for the design of both selective and dual-targeting inhibitors of CCR1 and CCR2, as a novel approach to treat inflammatory and immune diseases.

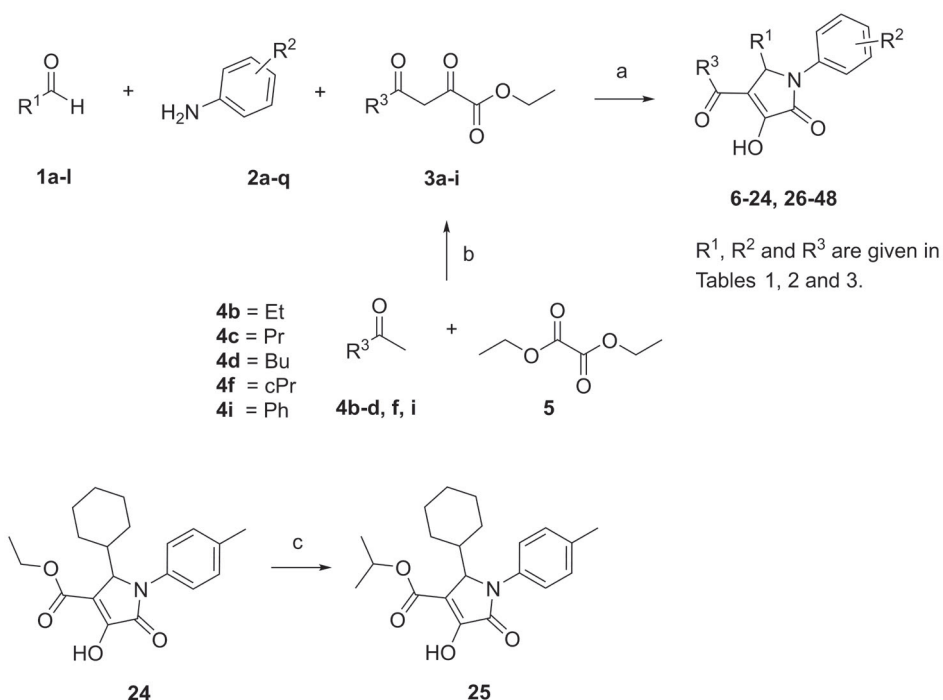
For CCR2, several compounds belonging to different scaffolds have already been reported to bind to this intracellular binding site, including pyrrolone derivatives such as CCR2-RA-[R], sulfonamide derivatives and 2-mercapto imidazoles.<sup>26, 28</sup> When tested for selectivity, some of these compounds also displayed a moderate activity on CCR1,<sup>29-31</sup> suggesting that they might also bind to CCR1. Thus, we selected the pyrrolone scaffold to explore a potential intracellular binding site in CCR1. In our current study, we report the synthesis and the biological evaluation of novel and previously patented pyrrolone derivatives<sup>32, 33</sup> at both CCR1 and CCR2, in order to determine their selectivity and structure-affinity relationships (SAR) for both receptors. Finally, compounds were tested in a [<sup>35</sup>S]GTPγS binding assay, in order to determine their functional effects in CCR1 and CCR2. Overall, our results provide evidence that CCR1 can also be targeted with intracellular allosteric modulators, and that this binding site can be used for the design of multi-target compounds.

## RESULTS AND DISCUSSION

### Synthesis of pyrrolone derivatives

The racemic pyrrolones (**6-24**, **26-46**) depicted in Scheme 1 were synthesized via a one pot three component condensation reaction, starting from the commercially available substituted aldehydes **1a-l**, anilines **2a-q** and ethyl 2,4-dioxo-butanoates **3a-i** in acetic acid<sup>33</sup> (**6-23**, **26-46**) or THF<sup>29</sup> (**24**). The ethyl 2,4-dioxo-butanoates (**3b-d**, **f**, **i**), which were not commercially available, were prepared by a Claisen condensation starting from the methyl ketones (**4b-d**, **f**, **i**) and diethyl oxalate **5**.<sup>34</sup> Pyrrolone **25** was prepared via a transesterification of **24** by the use of *p*-toluenesulfonic acid in 2-propanol.

**Scheme 1. Synthesis route of pyrrolones 6 – 48, with different R<sup>1</sup>, R<sup>2</sup> and R<sup>3</sup> substituents<sup>a</sup>**



<sup>a</sup>Reagents and conditions: (a) acetic acid, reflux for 2-4 h or THF, rt, overnight; (b) Na, EtOH, 0-20 °C, overnight; (c) *p*-toluenesulfonic acid, 2-propanol, reflux, 48 h.

## Characterization of [<sup>3</sup>H]-CCR2-RA-[R] binding on CCR1 and CCR2

[<sup>3</sup>H]-CCR2-RA-[R] is the (*R*)-isomer of [<sup>3</sup>H]-CCR2-RA, a high-affinity radioligand previously characterized in our group for CCR2.<sup>26</sup> To avoid a possible effect of the lower-affinity isomer, we used the tritium-labeled (*R*)-isomer in the present study. As expected, [<sup>3</sup>H]-CCR2-RA-[R] binds with high-affinity to osteosarcoma (U2OS) cells stably expressing CCR2b (U2OS-CCR2) as shown by saturation experiments ( $K_D$  of 6.3 nM and  $B_{max}$  of 2.6 pmol/mg, Figure S1 and Table S1). Kinetic characterization showed that [<sup>3</sup>H]-CCR2-RA-[R] associates and dissociates in a biphasic manner (Table S1), consistent with the previously reported [<sup>3</sup>H]-CCR2-RA kinetics.<sup>26</sup> We had reported that [<sup>3</sup>H]-CCR2-RA binds with low affinity to CCR5 ( $K_D$  of 100 nM),<sup>28</sup> suggesting that CCR2-RA-[R] is a non-selective antagonist that can bind several chemokine receptors. In this regard, CCR1 is a close homolog of CCR2, with 61% amino acid similarity and 47% identity; furthermore, this amino acid similarity is > 90% when only considering the amino acid residues involved in the intracellular binding site of CCR2-RA-[R] in CCR2 (**Chapters 2 and 3**)<sup>24, 27</sup> (Figure S2). This prompted us to investigate the binding of [<sup>3</sup>H]-CCR2-RA-[R] in membrane preparations from U2OS cells stably expressing CCR1 (U2OS-CCR1). [<sup>3</sup>H]-CCR2-RA-[R] homologous displacement assays on U2OS-CCR1 yielded a  $K_D$  of 13.5 nM and a  $B_{max}$  of 6.1 pmol/mg (Figure 1a, Table S1), suggesting the presence of an intracellular site in CCR1 and making it a suitable tool to study such binding pocket. Binding of [<sup>3</sup>H]-CCR2-RA-[R] to U2OS-CCR1 was also assessed in kinetic experiments at 25 °C. These experiments showed that [<sup>3</sup>H]-CCR2-RA-[R] associates and dissociates in a biphasic manner, similar to our findings in CCR2, but the association and dissociation rates were significantly higher in CCR1 than in CCR2 (Figure S1 and Table S1).

Overall, these findings allowed us to set up a [<sup>3</sup>H]-CCR2-RA-[R] competitive displacement assay on both U2OS-CCR1 and U2OS-CCR2, to determine the binding affinity ( $K_i$ ) of unlabeled compounds. Using this assay, we first determined the ability of known ligands to displace this radioligand from CCR1, i.e. the CCR2 intracellular ligands SD-24 and JNJ-27141491,<sup>26, 28</sup> and the CCR1 orthosteric antagonist BX471<sup>35</sup> (Figure 1b). SD-24 and JNJ-27141491 fully displaced [<sup>3</sup>H]-CCR2-RA-[R] from CCR1 in a concentration-dependent manner, indicating that these compounds bind at the same binding site as CCR2-RA-[R]. SD-24 displaced the radioligand with a  $pK_i$  of  $7.45 \pm 0.05$  ( $K_i = 36$  nM), while JNJ-27141491 displaced [<sup>3</sup>H]-CCR2-RA-[R] with a  $pK_i$  of  $6.9 \pm 0.06$  ( $K_i = 138$  nM), consistent with previously reported activities in CCR1.<sup>30, 31</sup> To rule out that these compounds bind at the orthosteric binding site of CCR1, we also investigated the effect of BX471 in [<sup>3</sup>H]-CCR2-RA-[R] binding. As expected, BX471 was not able to displace the radioligand (Figure 1b); on the contrary, BX471 significantly enhanced the binding of [<sup>3</sup>H]-CCR2-RA-[R] by approximately 20% ( $116 \pm 2\%$  in the presence of 10  $\mu$ M BX471), in a similar manner as previously reported with CCR2 orthosteric antagonists (**Chapter 3**).<sup>24, 26</sup> This allosteric enhancement is consistent with two different binding sites in



CCR1: the orthosteric binding site where BX471 binds and an intracellular pocket for CCR2-RA-[R], SD-24 and JNJ-27141491.

This [ $^3\text{H}$ ]-CCR2-RA-[R] assay was also used to determine the affinity of the synthesized pyrrolone derivatives. All pyrrolone derivatives **6** – **46** were first tested at a single concentration of 1  $\mu\text{M}$  in both U2OS-CCR1 and U2OS-CCR2 (Tables 1 – 3). Compounds which displaced more than 50% of [ $^3\text{H}$ ]-CCR2-RA-[R] binding were further evaluated in this assay using at least six different concentrations of unlabeled compound in order to determine their binding affinity for the corresponding receptor subtypes (Figures 1c,d and Tables 1 – 3). Finally, we selected four compounds (**39**, **41**, **43** and **45**) to be tested in a functional [ $^{35}\text{S}$ ] GTP $\gamma\text{S}$  binding assay (Figure 3). The potency ( $\text{pIC}_{50}$ ) of these compounds was determined in the presence of an  $\text{EC}_{80}$  concentration of CCL3 (8 nM) or CCL2 (20 nM) in U2OS-CCR1 or U2OS-CCR2 membranes, respectively.

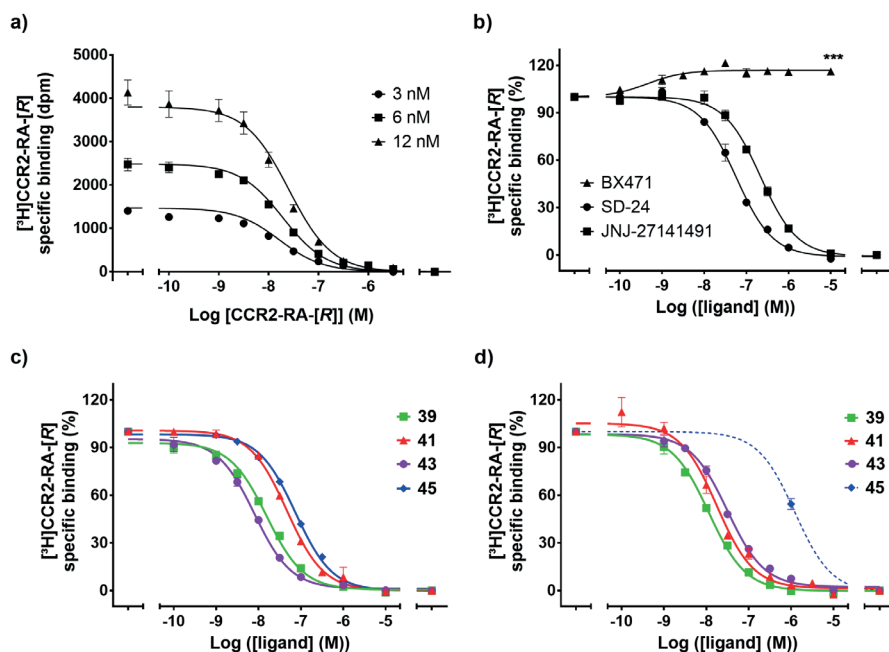


**Figure 1.** (a) Homologous displacement curves of 3, 6 and 12 nM [ $^3\text{H}$ ]-CCR2-RA-[R] specific binding by increasing concentrations of CCR2-RA-[R] in U2OS-CCR1, at 25°C. (b) Displacement curves of 6 nM [ $^3\text{H}$ ]-CCR2-RA-[R] specific binding by increasing concentrations of SD-24, JNJ-27141491 and BX471 in U2OS-CCR1 at 25°C. BX471 significantly enhanced the binding of [ $^3\text{H}$ ]-CCR2-RA-[R] up to 120%. Statistical significance between binding in absence (100%) and presence of 10  $\mu\text{M}$  BX471 ( $116 \pm 2\%$ ) was determined using an unpaired, two-tailed Student's *t*-test with Welch's correction. (c, d) Displacement curves of 6 nM [ $^3\text{H}$ ]-CCR2-RA-[R] specific binding by compounds **39**, **41**, **43** and **45** (c) in U2OS-CCR1 or (d) in U2OS-CCR2, at 25°C. In the case of U2OS-CCR2, compound **45** did not displace more than 50% of [ $^3\text{H}$ ]-CCR2-RA-[R], thus, only single-point data at 1  $\mu\text{M}$  is shown. The dashed blue line corresponds to the non-linear regression fit for compound **45** by GraphPad Prism 7.0. Data shown are mean  $\pm$  SEM of at least three experiments performed in duplicate.

## Docking of CCR2-RA-[R] in CCR1 and CCR2

In order to better understand the binding mode of CCR2-RA-[R] in both human CCR1 and CCR2b, we docked this compound into models of both receptors (Figure 2). In the case of CCR2, homology modeling was used to model the CCR2 residues between Ser226<sup>5x62</sup> and Lys240<sup>6x32</sup> (residues according to structure-based Ballesteros-Weinstein numbering<sup>36</sup>), which correspond to the M2 muscarinic acetylcholine receptor sequence in the CCR2b crystal structure (PDB ID:5T1A, **Chapter 3**).<sup>24</sup> These residues were modelled because this region is in close proximity to the CCR2-RA-[R] binding site. As expected from the sequence alignment (Figure S2), CCR2-RA-[R] was predicted to bind to CCR1 in an overlapping binding site as the one reported in the crystal structure of CCR2 (**Chapter 3**),<sup>24</sup> in a solvent-exposed intracellular pocket found between the intracellular ends of transmembrane segments 1 – 3, 6, 7 and helix 8 (Figure 2). The vinylogous carboxylic acid functionality makes similar interactions in CCR1 as in CCR2: the hydroxyl and the two carbonyl groups are involved in hydrogen-bond interactions with the side chain of Arg131<sup>3x50</sup>, and the backbone of Arg307<sup>8x49</sup> and Phe308<sup>8x50</sup> (Figure 2). A similar hydrophobic subpocket is also observed around the cyclohexyl moiety, which interacts with Ala<sup>6x33</sup>, Val/Leu<sup>6x36</sup>, Ile<sup>6x37</sup> and Ile<sup>6x40</sup>. Interestingly, Val244<sup>6x36</sup> in CCR2 is replaced by the bigger Leu240<sup>6x36</sup> in CCR1, which pushes the ligand down against Arg131<sup>3x50</sup>, resulting in a slightly different binding orientation of CCR2-RA-[R] in this receptor (Figure 2). In addition, the exchange of Lys311<sup>8x49</sup> in CCR2 by Arg307<sup>8x49</sup> in CCR1 might also contribute to the stabilization of this slightly altered binding pose. This difference in orientation could result in CCR1 selectivity, as this orientation seems to open up the subpockets in the proximity of the cyclohexyl and the acetyl group of CCR2-RA-[R] in CCR1, allowing the introduction of bigger and more lipophilic substituents at these positions.

## Structure-Affinity Relationships (SAR)

### *Modifications replacing the cyclohexyl group (R<sup>1</sup>, Table 1)*

Several pyrrolone derivatives have been previously evaluated at CCR2,<sup>29, 32, 33, 37</sup> resulting in the identification of CCR2-RA-[R] as a hit compound for further development,<sup>29</sup> but characterization of these compounds in CCR1 is mostly missing. Compound **6**, previously reported and characterized in CCR2 by Zou *et al.* (2007),<sup>37</sup> was selected as our starting point for the analysis of SAR in both CCR1 and CCR2. In our assay, compound **6** showed an affinity of 81 nM for CCR2, and a slightly higher affinity of 56 nM for CCR1 (Table 1). To note, the binding affinities reported previously for these pyrrolone derivatives were obtained with a <sup>125</sup>I-CCL2 binding assay,<sup>29, 37</sup> resulting in lower affinities compared with our [<sup>3</sup>H]-CCR2-RA-[R] binding assay, as previously observed in our group.<sup>26</sup> For our SAR study, we first examined

different C5 substituents of the pyrrolone core ( $R^1$ ), as shown in Table 1. In line with previous studies,<sup>29</sup> we found that increasing the size of the cycloalkyl group from cyclohexyl (**6**) to cycloheptyl (**7**) or cyclooctyl (**8**) resulted in a decrease in binding affinity for CCR2; however, the affinity for CCR1 was retained, indicating that bulkier groups are better tolerated in CCR1 than in CCR2, and providing an avenue for selectivity on CCR1 over CCR2. Previous studies showed that decreasing the size of the cycloalkyl group was also detrimental for CCR2,<sup>29</sup> so we decided not to explore smaller ring sizes.

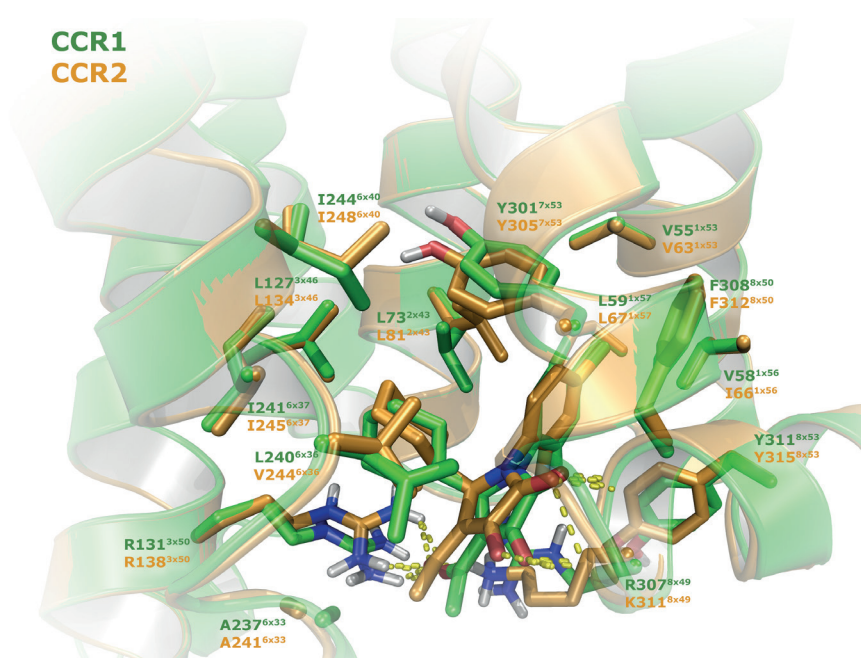


**Figure 2.** Proposed binding mode of compound CCR2-RA-[R] in the homology models of CCR1 and CCR2, based on the crystal structure of CCR2 (PDB ID: 5T1A, **Chapter 3**).<sup>24</sup> For CCR1 representative residues are shown as green ‘sticks’, and for CCR2 as orange ‘sticks’. In all cases, oxygen and nitrogen atoms are represented in red and blue, respectively; and hydrogen bonds with dashed yellow lines. Residues are numbered based on the corresponding residue numbers and with structure-based Ballesteros-Weinstein numbers in superscript.<sup>36</sup>

Substitution of the cycloalkyl group by a phenyl group (**9**) led to a great loss of CCR2 affinity (39% displacement at  $1\ \mu\text{M}$ ), consistent with previously reported values showing a decreased affinity for an almost similar pair of compounds.<sup>37</sup> Yet this substitution only led to a 3-fold decrease in CCR1 affinity ( $K_i$  of  $162\ \text{nM}$ ), thus showing much higher selectivity for CCR1. Next, we explored the effect of *N*-aryl modifications in both affinity and selectivity (compounds **10** – **17**), specifically the effect of para and meta substituents. In general, *N*-aryl groups on the  $R^1$  position resulted in increased selectivity towards CCR1, as most compounds did not displace more than 36% [ $^3\text{H}$ ]-CCR2-RA-[R] binding in CCR2 at a concentration of  $1\ \mu\text{M}$ . Only

compounds **12** and **13**, with halogen substitutions in para position (Cl and Br, respectively) regained CCR2 affinity (**12**, 207 nM; **13**, 214 nM). Furthermore, para-substituted derivatives displayed significantly higher affinities compared with their meta-substituted analogues.

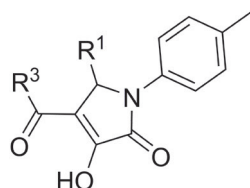
In the case of CCR1, introduction of a para-methyl moiety (**10**) resulted in a slight decrease in affinity compared with the unsubstituted **9**; in contrast, the meta-substituted analogue (**14**) showed less than 50% displacement at 1  $\mu$ M. Introduction of an electron-donating substituent (methoxy, **11** and **15**) was not well tolerated in any position, as it led to an approximately 3-fold decrease in affinity when placed in para position (**11**, 541 nM) and a near complete loss of affinity when placed in meta position (**15**, 28% displacement at 1  $\mu$ M). Halogen substituents in para position were also more favored in the case of CCR1, yielding higher affinities compared with the unsubstituted **9** and regardless of the halogen used (67 nM for R<sup>1</sup> = 4-Cl phenyl (**12**),  $p < 0.0001$  to **9**; 87 nM for R<sup>1</sup> = 4-Br phenyl (**13**);  $p = 0.0002$  to **9**). However, selectivity for CCR1 was notably reduced considering that these compounds displayed binding affinities of around 200 nM in CCR2. Although moving the halogens to the meta position (**16** and **17**) decreased the affinities more than 2-fold compared with their para analogues, selectivity for CCR1 was restored as these compounds showed less than 20% displacement of [<sup>3</sup>H]-CCR2-RA-[R] binding in CCR2. Together, the results for compounds **6** to **17** indicate that in CCR1 aliphatic groups yield higher affinities, while aromatic groups yield lower affinities but improved selectivity over CCR2.

### ***Modifications to the acetyl group (R<sup>3</sup>, Table 1)***

Previous modifications to the vinylogous carboxylic acid functionality in CCR2 showed detrimental effects in binding affinity.<sup>29, 37</sup> Indeed, mutagenesis and structural studies have shown crucial interactions of the hydroxyl and the two carbonyl groups with Glu310<sup>8x48</sup>, Lys311<sup>8x49</sup> and Phe312<sup>8x50</sup> in CCR2 (**Chapter 3**).<sup>24, 28</sup> Sequence alignment of CCR1 and CCR2 (Figure S2) and our docking study (Figure 2) suggest similar interactions in CCR1, as only position 8.49 differs (arginine in CCR1 and lysine in CCR2). Therefore, we decided to keep the vinylogous carboxylic acid moiety and explore different modifications to the acetyl group at the R<sup>3</sup> position (Table 1). A gradual increase in the length of the alkyl chain from a methyl group (**6**) to a butyl group (**18** – **20**) resulted in a ~2-fold increase in CCR1 affinity (30 nM for R<sup>3</sup> = ethyl (**18**),  $p = 0.0004$  against **6**; 29 nM for R<sup>3</sup> = propyl (**19**),  $p = 0.0002$  against **6**; and 31 nM for R<sup>3</sup> = butyl (**20**),  $p = 0.0010$  against **6**). In contrast, for CCR2 we observed a similar or a slight decrease in affinity. Introduction of a bulkier isopropyl group led to a decrease in affinity in both receptors, with a more drastic effect in CCR2 affinity. Replacing the isopropyl group with cyclopropyl (**22**) or *tert*-butyl (**23**) restored the affinity in CCR2 to values similar to compound **20** (**22**, 160 nM; **23**, 158 nM); in CCR1, these modifications further improved the binding affinity to approximately 20 nM, yielding compounds with the highest affinity

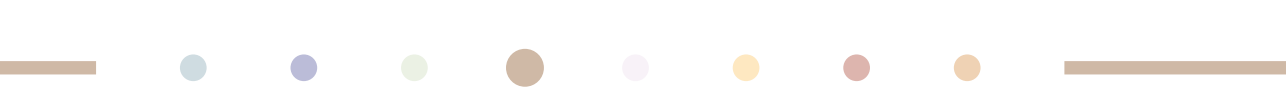
and selectivity observed in these series of R<sup>1</sup> and R<sup>3</sup> modifications (**22**, 19 nM; **23**, 22 nM). These results suggest a larger hydrophobic subpocket in CCR1, able to accommodate larger and branched alkyl chains.

**Table 1. Binding affinities of compounds 6 – 26 on human CCR1 and human CCR2.**



Compound	R <sup>1</sup>	R <sup>3</sup>	pK <sub>i</sub> ± SEM (K <sub>i</sub> , nM) <sup>a</sup> or displacement at 1 μM (%) <sup>b</sup>	
			CCR1	CCR2
<b>6</b>	c-hexyl	Me	7.26 ± 0.04 (56)	7.10 ± 0.03 (81)
<b>7</b>	c-heptyl	Me	7.26 ± 0.03 (56)	7.02 ± 0.06 (96)
<b>8</b>	c-octyl	Me	7.24 ± 0.01 (57)	6.79 ± 0.09 (170)
<b>9</b>	Ph	Me	6.79 ± 0.04 (162)	39% (38, 40)
<b>10</b>	4-Me Ph	Me	6.71 ± 0.06 (198)	36% (42, 31)
<b>11</b>	4-OMe Ph	Me	6.27 ± 0.01 (541)	5% (5, 5)
<b>12</b>	4-Cl Ph	Me	7.17 ± 0.01 (67)	6.70 ± 0.08 (207)
<b>13</b>	4-Br Ph	Me	7.07 ± 0.07 (87)	6.67 ± 0.04 (214)
<b>14</b>	3-Me Ph	Me	47% (51, 44)	11% (14, 8)
<b>15</b>	3-OMe Ph	Me	28% (34, 22)	0% (3, -3)
<b>16</b>	3-Cl Ph	Me	6.70 ± 0.01 (198)	19% (25, 14)
<b>17</b>	3-Br Ph	Me	6.74 ± 0.02 (181)	19% (20, 18)
<b>18</b>	c-hexyl	Et	7.52 ± 0.01 (30)	6.99 ± 0.06 (104)
<b>19</b>	c-hexyl	Pr	7.54 ± 0.04 (29)	6.86 ± 0.10 (144)
<b>20</b>	c-hexyl	Bu	7.50 ± 0.004 (31)	6.81 ± 0.05 (158)
<b>21</b>	c-hexyl	<i>i</i> -Pr	7.39 ± 0.06 (42)	6.50 ± 0.05 (316)
<b>22</b>	c-hexyl	<i>c</i> -Pr	7.74 ± 0.08 (19)	6.80 ± 0.05 (160)
<b>23</b>	c-hexyl	<i>t</i> -Bu	7.66 ± 0.05 (22)	6.81 ± 0.07 (158)
<b>24</b>	c-hexyl	OEt	6.70 ± 0.01 (200)	31% (36, 26)
<b>25</b>	c-hexyl	<i>O</i> /Pr	36% (45, 26)	6% (10, 1)
<b>26</b>	c-hexyl	-Ph	7.11 ± 0.01 (77)	37% (45, 30)

<sup>a</sup>pK<sub>i</sub> and K<sub>i</sub> (nM) values obtained from [<sup>3</sup>H]-CCR2-RA-[R] binding assays on U2OS membranes stably expressing human CCR1 or human CCR2. Values are means ± standard error of the mean (SEM) of at least three independent experiments performed in duplicate. <sup>b</sup>% of [<sup>3</sup>H]-CCR2-RA-[R] displacement by 1 μM compound. Values represent the mean of two independent experiments performed in duplicate.

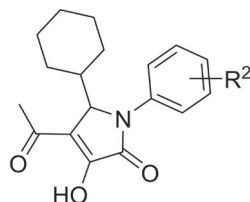


We also explored the effect of adding heteroatoms—oxygen in this case—between the carbonyl and an ethyl or isopropyl group (**24** and **25**, respectively). Overall, this led to a drastic drop in affinity for both receptors. This detrimental effect was most pronounced in compound **25**, which displaced less than 40% of [<sup>3</sup>H]-CCR2-RA-[R] binding in CCR1 and less than 10% in CCR2. The transformation of the ketone into an ester might decrease the electron density on the carbonyl oxygen, as well as the acidity of the adjacent protons, thus weakening or disrupting key hydrogen bonding interactions with Lys<sup>8x49</sup> in CCR2 (**Chapter 3**)<sup>24, 28</sup> or Arg<sup>8x49</sup> in CCR1. The need of an acidic function for intracellular antagonists has also been reported in a study with *N*-benzylindole-2-carboxylic acids, where the authors found a correlation between higher acidity and higher CCR2 affinity.<sup>38</sup> Finally, replacing the methyl group in R<sup>3</sup> with a phenyl group (**26**) had no effect on CCR1 affinity, while it only displaced 37% of [<sup>3</sup>H]-CCR2-RA-[R] binding in CCR2. Altogether these findings indicate that bigger, more lipophilic groups in R<sup>3</sup> are better tolerated in CCR1, while in CCR2 methyl is preferred.

### **Modifications to the phenyl ring (R<sup>2</sup>, Table 2)**

In addition, we explored different *N*-aryl modifications in the phenyl ring (R<sup>2</sup>, Table 2), starting with modifications in para position. Removing the methyl group in **6** yielded compound **27**, with an unsubstituted phenyl group, which displaced less than 50% of the radioligand in both receptors. Increasing the size of the alkyl group from methyl (**6**) to ethyl (**28**) caused a 3-fold decrease in CCR1 affinity, while the affinity in CCR2 was maintained (**28**, 168 nM in CCR1 versus 66 nM in CCR2). Adding an electron-donating methoxy group was unfavorable for both receptors, as affinities dropped to 260 nM in CCR1 and 217 nM in CCR2. In contrast, an electron-withdrawing substituent (trifluoromethyl, **32**) restored the affinity to 92 nM in CCR2, similar to our starting compound **6**, and to 144 nM in CCR1. The substitution of the para-methyl group with halogens yielded derivatives with improved binding affinities in both receptors (**30** and **31**), but no gain in selectivity. Substitution with a chlorine (**30**) or bromine atom (**31**) led to a 4.5-fold increase in CCR2 affinity compared with **6**, with K<sub>i</sub> values around 20 nM regardless of the halogen. In the case of CCR1, the bromine atom (**31**) led to a 2-fold increase compared with **6** (**31**, 24 nM), while the smaller chlorine atom did not affect the affinity much (**30**, 39 nM). Although not synthesized in our study, Dasse *et al.* (2007),<sup>29</sup> showed that the para-fluoro analogue performed worse in CCR2 than other para-halogen derivatives. In this regard, from fluoro to chloro there is an important increase in polarity ( $\sigma$ ), lipophilicity ( $\pi$ ) and size, whereas from chloro to bromo only lipophilicity and size increase.<sup>39, 40</sup> Taken together, these results suggest that lipophilicity and size of the halogen might be more important in CCR1 than in CCR2, while electronegativity or polarity could play a bigger role in CCR2.

**Table 2. Binding affinities of compounds 6, 27 – 42 on human CCR1 and human CCR2.**

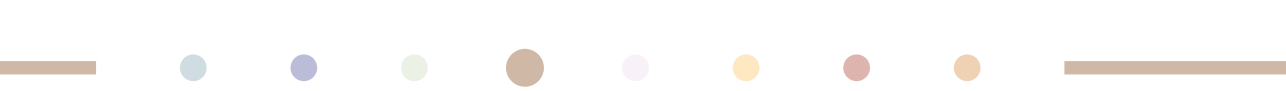


Compound	R <sup>2</sup>	pK <sub>i</sub> ± SEM (K <sub>i</sub> , nM) <sup>a</sup> or displacement at 1 μM (%) <sup>b</sup>	
		CCR1	CCR2
<b>27</b>	H	42% (41, 42)	45% (44, 45)
<b>6</b>	4-Me	7.26 ± 0.04 (56)	7.10 ± 0.03 (81)
<b>28</b>	4-Et	6.78 ± 0.02 (168)	7.19 ± 0.05 (66)
<b>29</b>	4-OMe	6.60 ± 0.07 (260)	6.67 ± 0.05 (217)
<b>30</b>	4-Cl	7.41 ± 0.05 (40)	7.73 ± 0.08 (19)
<b>31</b>	4-Br	7.62 ± 0.05 (24)	7.80 ± 0.12 (17)
<b>32</b>	4-CF <sub>3</sub>	6.86 ± 0.08 (144)	7.04 ± 0.02 (92)
<b>33</b>	3-Me	6.31 ± 0.07 (500)	6.58 ± 0.06 (265)
<b>34</b>	3-F	44% (45, 42)	47% (48, 47)
<b>35</b>	3-Cl	6.28 ± 0.08 (541)	6.62 ± 0.02 (239)
<b>36</b>	3-CF <sub>3</sub>	25% (23, 27)	6.54 ± 0.11 (305)
<b>37</b>	2-F, 4-Me	7.56 ± 0.10 (29)	7.44 ± 0.05 (37)
<b>38 (CCR2-RA)</b>	2-F, 4-Cl	7.82 ± 0.06 (15)	8.00 ± 0.09 (11)
<b>39</b>	2-F, 4-Br	7.98 ± 0.04 (11)	8.25 ± 0.02 (6)
<b>40</b>	3,4-diMe	7.37 ± 0.03 (43)	7.75 ± 0.02 (18)
<b>41</b>	3-Me, 4-Cl	7.51 ± 0.01 (31)	8.09 ± 0.08 (9)
<b>42</b>	3-F, 4-Me	7.32 ± 0.07 (49)	7.24 ± 0.02 (57)

<sup>a</sup>pK<sub>i</sub> and K<sub>i</sub> (nM) values obtained from [<sup>3</sup>H]-CCR2-RA-[R] binding assays on U2OS membranes stably expressing human CCR1 or human CCR2. Values are means ± standard error of the mean (SEM) of at least three independent experiments performed in duplicate. <sup>b</sup>% of [<sup>3</sup>H]-CCR2-RA-[R] displacement by 1 μM compound. Values represent the mean of two independent experiments performed in duplicate.

Moving the substituents from the para to the meta position resulted in poor affinities for both receptors, compared with their para-substituted analogues. In CCR1, the *meta*-methyl (**33**) and *meta*-chlorine (**35**) groups led to a 9-fold and 13-fold decrease in affinity, respectively; in CCR2, the affinities decreased 3-fold and 13-fold after the same substitutions. The addition of a trifluoromethyl group in meta position (**36**) also led to a 3-fold decrease in CCR2 affinity compared with its para-substituted analogue **32**. In CCR1 **36** only displaced 25% of [<sup>3</sup>H]-CCR2-RA-[R] binding at a concentration of 1 μM, displaying the highest selectivity towards





CCR2 in these series of modifications. Also detrimental was the addition of a fluorine group in meta position (**34**), which led to less than 50% displacement of [<sup>3</sup>H]-CCR2-RA-[R] binding in both receptors. Overall, substituents in para position were more favored in both receptors, especially halogen substituents, yet none of the compounds displayed selectivity towards CCR1. Similarly as reported by Dasse *et al.* (2007),<sup>29</sup> attempts to introduce different substituents in the ortho position were unsuccessful, thus we continued to explore different combinations of phenyl substituents.

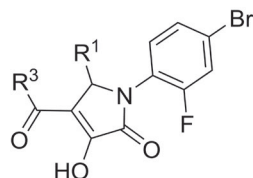
As part of our SAR analysis we synthesized compound **38** (also referred as CCR2-RA), which corresponds to the racemic mixture of the radioligand [<sup>3</sup>H]-CCR2-RA-[R] used in this study. This compound displayed an affinity of 15 nM in CCR1 and 10 nM in CCR2, similar to the  $K_d$  values obtained in homologous displacement or saturation assays (Table S1). Replacing the para-chloro group in **38** with a methyl moiety (**37**), while keeping the ortho-fluorine group, led to an expected decrease in affinity for both receptors, as compound **6** with a methyl group in para position performed worse than **30** with a chlorine atom in the same position. When the para substituent was replaced with a bromine atom (**39**), the affinity was restored to 11 nM in CCR1 and 6 nM in CCR2. Subsequent combinations of meta and para substituents (**40 – 42**) generated compounds with decreased CCR1 affinities compared with **38**, as expected from the data on the mono-substituted meta analogues. Compound **41** displayed a slightly higher selectivity for CCR2 (8 nM in CCR2 *versus* 31 nM in CCR1). Overall, disubstituted derivatives performed better than the mono-substituted compounds in both receptors; however, no clear trend in selectivity was observed in these series.

In an attempt to improve both affinity and selectivity for CCR1, we decided to combine some of the best features observed at R<sup>1</sup>, R<sup>2</sup> and R<sup>3</sup> positions: a disubstituted phenyl ring with an ortho-fluoro and para-bromo moieties for R<sup>2</sup>, in order to retain the high affinity of **39**; a cyclopropyl group or an unsubstituted phenyl ring at R<sup>3</sup> (**22** and **26**) to gain selectivity; and a meta-bromo phenyl ring at R<sup>1</sup> (**17**) to further improve selectivity for CCR1. These combinations resulted in four final compounds shown in Table 3 (**43 – 46**). To maintain a high affinity for CCR1, we kept the 2-fluoro-4-bromophenyl group at R<sup>2</sup> constant and we combined it with different R<sup>1</sup> and R<sup>3</sup> substituents. The combination with a cyclopropyl group at R<sup>3</sup> position (**43**) led to the highest CCR1 affinity in our study ( $K_i$  of 5 nM), but selectivity over CCR2 was reduced compared with **22** (3-fold *versus* 8-fold). Replacing the cyclopropyl group at R<sup>3</sup> by a phenyl group (**44**) decreased the affinity for CCR1 by more than 5-fold compared with **43**. Compound **43**, somewhat unexpectedly, bound to CCR2 with an affinity of 66 nM, more than 15-fold better than **26**. Replacing the cyclohexyl group at R<sup>1</sup> (**43**) by a 3-bromo-phenyl group (**45**) resulted in an improved selectivity over CCR2, as this compound did not displace more than 50% of [<sup>3</sup>H]-CCR2-RA-[R] binding at 1 μM, whereas it showed an affinity of 50 nM in CCR1. Finally, replacing the cyclopropyl with a methyl group at R<sup>3</sup> (**46**)



maintained the affinity for CCR1 and restored the affinity for CCR2 (65 nM in CCR1 and 216 nM in CCR2), with a concomitant loss of selectivity.

**Table 3. Binding affinities of compounds 43 – 46 on human CCR1 and human CCR2.**



Compound	R <sup>1</sup>	R <sup>3</sup>	pK <sub>i</sub> ± SEM (K <sub>i</sub> , nM) <sup>a</sup> or displacement at 1 μM (%) <sup>b</sup>	
			CCR1	CCR2
<b>43</b>	c-hexyl	c-propyl	8.27 ± 0.02 (5)	7.82 ± 0.04 (15)
<b>44</b>	c-hexyl	Ph	7.56 ± 0.04 (28)	7.18 ± 0.03 (66)
<b>45</b>	3-Br Ph	c-propyl	7.30 ± 0.01 (50)	45% (49, 42)
<b>46</b>	3-Br Ph	Me	7.19 ± 0.02 (65)	6.67 ± 0.01 (216)

<sup>a</sup>pK<sub>i</sub> and K<sub>i</sub> (nM) values obtained from [<sup>3</sup>H]-CCR2-RA-[R] binding assays on U2OS membranes stably expressing human CCR1 or human CCR2. Values are means ± standard error of the mean (SEM) of at least three independent experiments performed in duplicate. <sup>b</sup>% of [<sup>3</sup>H]-CCR2-RA-[R] displacement by 1 μM compound. Values represent the mean of two independent experiments performed in duplicate.

## Functional characterization of selected compounds

Following the SAR analysis, four compounds (**39**, **41**, **43** and **45**) were selected for further characterization in a G protein-dependent functional assay, in order to assess their inhibitory potencies (pIC<sub>50</sub>) in both CCR1 and CCR2. The four compounds were selected based on their affinity and selectivity profile: compounds **43** and **39**, with the highest affinity for either CCR1 or CCR2 respectively; compound **41**, with higher selectivity towards CCR2; and compound **45**, with higher selectivity towards CCR1. As functional assay we used a previously reported [<sup>35</sup>S]GTPγS binding assay on U2OS-CCR2 membranes, which had been applied in the functional characterization of several allosteric and orthosteric CCR2 ligands.<sup>26</sup> Similarly as reported by Zweemer *et al.* (2013),<sup>26</sup> CCL2 stimulated [<sup>35</sup>S]GTPγS binding in a concentration-dependent manner, displaying a potency of 5 nM in CCR2 (pEC<sub>50</sub> = 8.3 ± 0.09, Figure 3a). Using the same assay conditions, we characterized the G protein activation of CCL3 in U2OS-CCR1 membranes. In this assay, CCL3 induced [<sup>35</sup>S]GTPγS binding in CCR1 with a higher potency than CCL2 in CCR2 (1.3 nM, pEC<sub>50</sub> = 8.9 ± 0.06), and with a higher maximum effect (*E*<sub>max</sub>) (Figure 3a). It should be noted that the potency of CCL3 in our study is lower than previously reported,<sup>41</sup> which might be related to the differences in cell line and/or assay conditions.

For the antagonist assays, we used a submaximal EC<sub>80</sub> concentration of CCL3 (8 nM) and CCL2 (20 nM) in CCR1 or CCR2, respectively, in order to evoke 80% stimulation of [<sup>35</sup>S]GTPγS binding. Although all compounds were able to inhibit CCL3- or CCL2-induced G protein activation, their potencies (IC<sub>50</sub>) ranged between 30 nM to 8 μM (Table 4 and Figure 3b,c). In CCR2, the potency of the compounds increased in the same order observed for affinity (Figure 3c, **45** < **43** < **41** < **39**). In CCR1 **39** displayed the highest potency (590 nM), followed by **43** (950 nM), contrary to their binding affinity (Figure 3b, **43** > **39**). In addition, the moderate selectivity observed in the binding assays was lost in this functional assay: except for **45**, all compounds were more potent inhibitors of CCR2 than CCR1, as their potencies were 3-fold (**43**), 19-fold (**39**) or 48-fold (**41**) lower in CCR1. Upon comparison of potencies in the [<sup>35</sup>S]GTPγS assay and the affinities in the [<sup>3</sup>H]-CCR2-RA-[R] binding assay, we observed that all compounds displayed between 5 to 10-fold difference between assays in CCR2 (Tables 2 – 4), in agreement with previous characterization of CCR2-RA-[R] on this receptor.<sup>26</sup> In contrast, all compounds displayed at least a 50-fold difference between assays when tested on CCR1. Such lack of correlation between apparent potencies and binding affinities in CCR1 might be dependent on the assay conditions used, G protein concentrations, or the chemokine used in this study; thus, further studies are warranted to fully characterize these ligands for their selectivity.

**Table 4. Functional characterization of compounds 37, 39, 41 and 43 in U2OS-CCR1 and U2OS-CCR2 using a [<sup>35</sup>S]GTPγS binding assay.**

Compound	Inhibition of [ <sup>35</sup> S]GTPγS binding <sup>a</sup>					
	CCR1 <sup>b</sup>			CCR2 <sup>c</sup>		
	pIC <sub>50</sub> ± SEM	(IC <sub>50</sub> , μM)	Hill slope	pIC <sub>50</sub> ± SEM	(IC <sub>50</sub> , μM)	Hill slope
<b>39</b>	6.26 ± 0.10	(0.59)***	-0.62 ± 0.05**	7.57 ± 0.08	(0.03)	-0.94 ± 0.18
<b>41</b>	5.73 ± 0.09	(1.94)***	-0.72 ± 0.08*	7.47 ± 0.10	(0.04)	-0.88 ± 0.13
<b>43</b>	6.03 ± 0.04	(0.95)	-0.73 ± 0.02*	6.54 ± 0.16	(0.33)	-0.80 ± 0.13
<b>45</b>	5.07 ± 0.05	(8.64)	-0.93 ± 0.01	5.06 ± 0.05	(8.77)	-1.20 ± 0.08

<sup>a</sup>All values are means ± SEM. of at least three independent experiments performed in duplicate. Unpaired *t*-test analysis with Welch's correction was performed to analyze differences in pIC<sub>50</sub> values between receptors, with differences noted as \*\*\*, *p* < 0.001. One-way ANOVA with Dunnett's post-hoc test was performed to compare pseudo-Hill slopes against compound **45**, which showed a pseudo-Hill slope of approx. unity in both receptors, with significant differences displayed as \*, *p* < 0.05; \*\*, *p* < 0.01. <sup>b</sup>Inhibition of CCL3-induced [<sup>35</sup>S]GTPγS binding in U2OS membranes stably expressing human CCR1. A concentration of 8 nM CCL3 was used in the assays to evoke an 80% response. <sup>c</sup>Inhibition of CCL2-induced [<sup>35</sup>S]GTPγS binding in U2OS membranes stably expressing human CCR2. A concentration of 20 nM CCL2 was used in the assays to evoke an 80% response.

In CCR1, all compounds behaved as inverse agonists, as they all significantly decreased the basal activity of CCR1 at the highest concentration tested (Figure S3a). In this regard, it was previously demonstrated that CCR1 exhibits constitutive activity leading to ligand-independent G protein-activation,  $\beta$ -arrestin recruitment and receptor internalization,<sup>42</sup> which points to the development of inverse agonists as a potential therapeutic option for inflammatory diseases. Yet, only BX471<sup>35</sup> has been reported to act as inverse agonist in CCR1.<sup>42</sup> This prompted us to further characterize these compounds as inverse agonists in CCR1, by measuring their inhibitory potency in absence of the agonist CCL3 (Figure S3b and Table S2). Compounds **39** and **41** were more potent inverse agonists than antagonists, displaying a 3-fold and almost 10-fold higher potency, respectively, as inverse agonists. As such, their potencies as inverse agonists were more comparable to their binding affinities (Table 2 and Table S2). In contrast, **43** and **45** showed similar potencies when measured in the absence or presence of CCL3, and thus, displayed more than 130-fold difference between functional and binding assays (Table 2 and Table S2). Interestingly, both compounds **43** and **45** have a cyclopropyl in the R<sup>3</sup> position while **39** and **41** have a methyl group (Tables 2 and 3), which suggests that this larger group might be responsible for the difference in their efficacy and functional profile. Moreover, most compounds displayed pseudo-Hill slopes of less than unity in CCR1, when tested in the presence or absence of CCL3 (Table 4 and Table S2), indicative of a more complex mechanism of inhibition, combining negative allosteric modulation and inverse agonism.<sup>43</sup> Of note, the basal levels of constitutive activity in the [<sup>35</sup>S]GTP $\gamma$ S assay are very dependent on the assay conditions used, such as GDP concentrations. Yet, at a single-concentration (100  $\mu$ M) tested, all compounds consistently decreased the basal activity in CCR1 after varying GDP concentrations. For instance, compound **41** decreased basal activity by 22% (1  $\mu$ M GDP), 26% (10  $\mu$ M GDP) and 25% (20  $\mu$ M GDP) (data not shown). To the best of our knowledge, these compounds represent the first intracellular ligands with demonstrated inverse agonism in CCR1. Both **45** and **43** decreased the basal activity of CCR2 to a similar or smaller level than in CCR1 (**45**, maximal decrease of 58%; **43**, maximal decrease of 27%), indicative of inverse agonism (Figure S3a). However, no constitutive activity has been reported for CCR2, with only one constitutively active mutant (CAM) described so far.<sup>44</sup> In fact, Gilliland *et al.* (2013) showed that CCR2 was not able to induce ligand-independent cell migration or to constitutively associate with  $\beta$ -arrestin, pointing to a lack of constitutive activity.<sup>42</sup> Moreover, several classes of orthosteric and allosteric CCR2 ligands did not show evidence of inverse agonism when previously tested in a similar [<sup>35</sup>S]GTP $\gamma$ S binding assay.<sup>26</sup> Thus, the inverse agonism observed in this study might be the consequence of the expression level, ligand concentration and/or assay conditions employed, so further research is warranted to investigate ligand-independent signaling in CCR2.

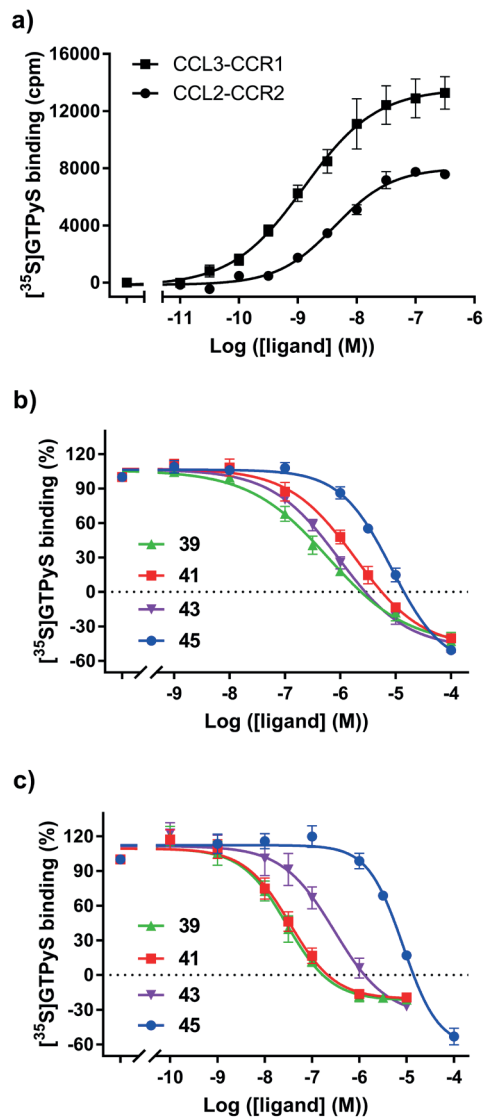


**Figure 3.** (a)  $[^{35}\text{S}]\text{GTP}\gamma\text{S}$  binding upon stimulation of U2OS-CCR1 and U2OS-CCR2 by increasing concentrations of CCL3 and CCL2, respectively. In both cases, the response was corrected by subtracting the basal activity (approx. 8000 dpm for both CCR1 and CCR2). (b) Inhibition of CCL3-induced  $[^{35}\text{S}]\text{GTP}\gamma\text{S}$  binding by compounds **39**, **41**, **43** and **45** in U2OS-CCR1. (c) Inhibition of CCL2-induced  $[^{35}\text{S}]\text{GTP}\gamma\text{S}$  binding by compounds **39**, **41**, **43** and **45** in U2OS-CCR2. The level of basal activity in U2OS-CCR1 and U2OS-CCR2 is indicated by a dashed line. In all cases data shown are mean  $\pm$  SEM of at least three experiments performed in duplicate.

## CONCLUSIONS

In this study we have characterized [<sup>3</sup>H]-CCR2-RA-[R], a high-affinity intracellular antagonist previously described for CCR2,<sup>26</sup> in both CCR1 and CCR2, which allowed us to conclude that this radioligand binds to CCR1 with a similar high-affinity. By characterizing this radioligand in CCR1, we have provided evidence that CCR1 possesses an intracellular binding site that can be used for the design of non-competitive compounds. In addition, this intracellular radioligand allowed us to explore the SAR of a series of pyrrolone derivatives in both CCR1 and CCR2. Although some of these derivatives had been previously described for CCR2, their characterization in CCR1 had not been reported. With the SAR analysis we learned that introduction of bulkier and more lipophilic groups at R<sup>1</sup> and R<sup>3</sup> positions was better tolerated in CCR1, allowing us to obtain better selectivity for this receptor. The high conservation between the intracellular pockets of CCR1 and CCR2 prevented us from finding high selectivity in these series of compounds, but allowed us to find several potential dual-target antagonists. Finally, characterization of four selected compounds in a functional assay allowed us to determine their functional effects as antagonists in CCR2 and inverse agonists in the constitutively-active CCR1, which opens up a novel avenue to modulate these receptors in inflammatory diseases. In addition, this highly-conserved binding site might allow the design of both selective and multi-target inhibitors for chemokine receptors, beyond CCR1 and CCR2.

## EXPERIMENTAL SECTION

### Chemistry

#### General methods.

All solvents and reagents were purchased from commercial sources and were of analytical grade. Demineralized water is simply referred to as H<sub>2</sub>O, as was used in all cases unless stated otherwise (i.e. brine). <sup>1</sup>H NMR spectra were recorded on a Bruker AV 400 liquid spectrometer (<sup>1</sup>H NMR, 400 MHz) at ambient temperature. Chemical shifts are reported in parts per million (ppm), are designated by  $\delta$  and are downfield to the internal standard tetramethylsilane (TMS) in CDCl<sub>3</sub>. Coupling-constants are reported in Hz and are designated as *J*. As a representative example of the obtained <sup>1</sup>H NMR spectra, Figure S4 shows the <sup>1</sup>H NMR spectrum of compound **43**. Analytical purity of the final compounds was determined by high pressure liquid chromatography (HPLC) with a Phenomenex Gemini 3 × C18 110A column (50 × 4.6 mm, 3  $\mu$ m), measuring UV absorbance at 254 nm. Sample preparation and HPLC method was—unless stated otherwise—as follows: 0.3–0.8 mg of compound was dissolved in 1 mL of a 1:1:1 mixture of CH<sub>3</sub>CN/H<sub>2</sub>O/tBuOH and eluted from the column within 15 min, with a three component system of H<sub>2</sub>O/CH<sub>3</sub>CN/1% TFA in H<sub>2</sub>O, decreasing polarity of the solvent mixture in time from 80/10/10 to 0/90/10. All compounds showed a single peak at the designated retention time and are at least 95% pure. Liquid chromatography–mass spectrometry (LC–MS) analyses were performed using Thermo Finnigan Surveyor – LCQ Advantage Max LC–MS system and a Gemini C18 Phenomenex column (50 × 4.6 mm, 3  $\mu$ m). The elution method was set up as follows: 1–4 min isocratic system of H<sub>2</sub>O/CH<sub>3</sub>CN/1% TFA in H<sub>2</sub>O, 80:10:10, from the 4th min, a gradient was applied from 80:10:10 to 0:90:10 within 9 min, followed by 1 min of equilibration at 0:90:10 and 1 min at 80:10:10. Thin-layer chromatography (TLC) was routinely performed to monitor the progress of reactions, using aluminum coated Merck silica gel F254 plates. Purification by column chromatography was achieved by use of Grace Davison DAVISIL silica column material (LC60A 30–200 micron). Yields and reaction conditions were not optimized. Additionally, all compounds were screened using FAF-Drugs<sup>45, 46</sup> in order to detect potential Pan-Assay Interference Compounds (PAINS). None of the compounds was identified as PAINS after application of three different filters based on Baell *et al.*<sup>47</sup>

## General procedure for the synthesis of compounds 6 – 23, 26 – 46.<sup>33</sup>

The respective aldehyde **1a-l** (1.0 eq.), aniline **2a-q** (1.0 eq.) and ethyl 2,4-dioxo-butanoate analogue **3a-i** (1.0 eq.) were dissolved in acetic acid (2.5 mL/mmol) and heated at 95°C for 2-4 h under a nitrogen atmosphere. Upon completion of the reaction (TLC 1/7 EtOAc/Pet ether) acetic acid was removed under reduced pressure, the residue was triturated with Et<sub>2</sub>O and stirred for 30 minutes after which the pure product was collected by filtration.

### 4-Acetyl-5-cyclohexyl-3-hydroxy-1-(4-methylphenyl)-1,5-dihydro-2H-pyrrol-2-one (**6**).<sup>33</sup>

Started from cyclohexane carboxaldehyde **1a** (243  $\mu$ L, 2.00 mmol, 1.00 eq.), 4-methylaniline (214 mg, 2.00 mmol, 1.00 eq.) and ethyl 2,4-dioxopentanoate **3a** (251  $\mu$ L, 2.00 mmol, 1.00 eq.) in 5 mL of acetic acid. Yield: 287 mg, 46%, white solid. <sup>1</sup>H NMR (400 MHz, DMSO):  $\delta$  7.38 (d,  $J$  = 8.4 Hz, 2H), 7.24 (d,  $J$  = 8.4 Hz, 2H), 4.99 (d,  $J$  = 1.2 Hz, 1H), 2.43 (s, 3H), 2.32 (s, 3H), 1.83 (t,  $J$  = 11.2 Hz, 1H), 1.65-1.56 (m, 1H), 1.52-1.27 (m, 4H), 0.53 (qd,  $J$  = 12.4, 2.8 Hz, 1H) ppm. MS [ESI+H]<sup>+</sup>: 313.93.

### 4-Acetyl-5-cycloheptyl-3-hydroxy-1-(4-methylphenyl)-1,5-dihydro-2H-pyrrol-2-one (**7**).<sup>32</sup>

Started from cycloheptylcarboxaldehyde **1b**<sup>48</sup> (375 mg, 3.00 mmol, 1.00 eq.), 4-methylaniline **2b** (321 mg, 3.00 mmol, 1.00 eq.) and ethyl 2,4-dioxopentanoate **3a** (377  $\mu$ L, 3.00 mmol, 1.00 eq.) in 7.5 mL of acetic acid. Purified by recrystallization from a mixture of EtOAc and Pet. Ether. Yield: 102 mg, 13%, off-white solid. <sup>1</sup>H NMR (400 MHz, CDCl<sub>3</sub>):  $\delta$  7.26-7.22 (m, 4H), 4.95 (d,  $J$  = 1.6 Hz, 1H), 2.54 (s, 3H), 2.38 (s, 3H) ppm, 2.09-2.03 (m, 1H), 1.61-1.47 (m, 4H), 1.46-1.32 (m, 4H), 1.31-1.12 (m, 4H), 0.80 (qd,  $J$  = 10.8, 3.2 Hz, 1H) ppm. MS: [ESI+H]<sup>+</sup>: 328.13.

### 4-Acetyl-5-cyclooctyl-3-hydroxy-1-(4-methylphenyl)-1,5-dihydro-2H-pyrrol-2-one (**8**).<sup>32</sup>

Started from cyclooctylcarboxaldehyde **1c** (648 mL, 4.42 mmol, 1.00 eq.), 4-methylaniline **2b** (474 mg, 4.42 mmol, 1.00 eq.) and ethyl 2,4-dioxopentanoate **3a** (554  $\mu$ L, 4.42 mmol, 1.00 eq.) in 10 mL of acetic acid. Purified by column chromatography using as eluent 1/6 EtOAc/Pet ether. Yield: 118 mg, 8%, white solid. <sup>1</sup>H NMR (400 MHz, CDCl<sub>3</sub>):  $\delta$  7.26-7.21 (m, 4H), 4.90 (d,  $J$  = 1.6 Hz, 1H), 2.53 (s, 3H), 2.37 (s, 3H), 2.22-2.14 (m, 1H), 1.62-1.52 (m, 1H), 1.50-1.15 (m, 13H) 0.89-0.78 (m, 1H) ppm. MS: [ESI+H]<sup>+</sup>: 342.20.

### 4-Acetyl-3-hydroxy-1-(4-methylphenyl)-5-phenyl-1,5-dihydro-2H-pyrrol-2-one (**9**).<sup>32</sup>

Started from benzaldehyde **1d** (449 mL, 4.42 mmol, 1.00 eq.), 4-methylaniline **2b** (474 mg, 4.42 mmol, 1.00 eq.) and ethyl 2,4-dioxopentanoate **3a** (554  $\mu$ L, 4.42 mmol, 1.00 eq.) in 10 mL of acetic acid. Yield: 867 mg, 64%, off-white solid. <sup>1</sup>H NMR (400 MHz, CDCl<sub>3</sub>):  $\delta$  7.28-7.24 (m, 5H), 7.22 (d,  $J$  = 6.0 Hz, 2H), 7.07 (d,  $J$  = 8.0 Hz, 2H), 5.75 (s, 1H), 2.49 (s, 3H), 2.16 (s, 3H) ppm. MS [ESI+H]<sup>+</sup>: 308.00.

**4-Acetyl-3-hydroxy-5-(4-methylphenyl)-1-(4-methylphenyl)-1,5-dihydro-2H-pyrrol-2-one (**10**)**. Started from 4-methylbenzaldehyde **1e** (521 mL, 4.42 mmol, 1.00 eq.), 4-methylaniline **2b** (474 mg, 4.42 mmol, 1.00 eq.) and ethyl 2,4-dioxopentanoate **3a** (554  $\mu$ L, 4.42 mmol, 1.00 eq.) in 10 mL of acetic acid. Purified by recrystallization from acetone/hexanes. Yield: 257 mg, 18% yellowish solid. <sup>1</sup>H NMR (400 MHz, DMSO-*d*<sub>6</sub>):  $\delta$  7.42 (d,  $J$  = 8.4 Hz, 2H), 7.12-7.04 (m, 4H), 6.98 (d,  $J$  = 8.0 Hz, 2H), 5.94 (s, 1H), 2.30 (s, 3H), 2.19 (s, 3H), 2.16 (s, 3H) ppm. MS [ESI+H]<sup>+</sup>: 322.00.

**4-Acetyl-3-hydroxy-5-(4-methoxyphenyl)-1-(4-methylphenyl)-1,5-dihydro-2H-pyrrol-2-one (**11**)**.<sup>49</sup> Started from 4-methoxybenzaldehyde **1f** (527 mL, 4.42 mmol, 1.00 eq.), 4-methylaniline **2b** (474 mg, 4.42 mmol, 1.00 eq.) and ethyl 2,4-dioxopentanoate **3a** (554  $\mu$ L, 4.42 mmol, 1.00 eq.) in 10 mL of acetic acid. The desired product was obtained by column chromatography using a gradient of 1/6 EtOAc/Pet Ether to 1/3 EtOAc/Pet Ether, yielding 34 mg, 2% as an off-white solid. <sup>1</sup>H NMR (400 MHz, DMSO-*d*<sub>6</sub>):  $\delta$  7.42 (d,  $J$  = 8.4 Hz, 2H), 7.12 (d,  $J$  = 8.4 Hz, 2H), 7.08 (d,  $J$  = 8.8 Hz, 2H), 6.73 (d,  $J$  = 8.8 Hz, 2H) 5.93 (s, 1H), 3.64 (s, 3H), 2.30 (s, 3H), 2.20 (s, 3H) ppm. MS [ESI+H]<sup>+</sup>: 337.80.

**4-Acetyl-5-(4-chlorophenyl)-3-hydroxy-1-(4-methylphenyl)-1,5-dihydro-2H-pyrrol-2-one (12).**<sup>32</sup> Started from 4-chlorobenzaldehyde **1g** (621 mg, 4.42 mmol, 1.00 eq.), 4-methylaniline **2b** (474 mg, 4.42 mmol, 1.00 eq.) and ethyl 2,4-dioxopentanoate **3a** (554  $\mu$ L, 4.42 mmol, 1.00 eq.) in 10 mL of acetic acid. The desired product was obtained by column chromatography using 1/6 EtOAc/Pet ether as eluent, yielding 96 mg, 6% as a white solid. <sup>1</sup>H NMR (400 MHz, DMSO-*d*<sub>6</sub>):  $\delta$  7.43 (d, *J* = 8.4 Hz, 2H), 7.30-7.18 (m, 4H), 7.08 (d, *J* = 8.4 Hz, 2H), 5.98 (s, 1H), 2.30 (s, 3H), 2.20 (s, 3H) ppm. MS [ESI+H]<sup>+</sup>: 342.00.

**4-Acetyl-5-(4-bromophenyl)-3-hydroxy-1-(4-methylphenyl)-1,5-dihydro-2H-pyrrol-2-one (13).**<sup>32</sup> Started from 4-bromobenzaldehyde **1h** (818 mg, 4.42 mmol, 1.00 eq.), 4-methylaniline **2b** (474 mg, 4.42 mmol, 1.00 eq.) and ethyl 2,4-dioxopentanoate **3a** (554  $\mu$ L, 4.42 mmol, 1.00 eq.) in 10 mL of acetic acid. Yield: 1.23 g, 72%, yellowish solid. <sup>1</sup>H NMR (400 MHz, CDCl<sub>3</sub>):  $\delta$  7.39 (d, *J* = 8.8 Hz, 2H), 7.25 (d, *J* = 8.8 Hz, 2H), 7.11-7.08 (m, 4H), 5.73 (s, 1H), 2.27 (s, 3H), 2.23 (s, 3H) ppm. MS [ESI+H]<sup>+</sup>: 387.93.

**4-Acetyl-3-hydroxy-5-(3-methylphenyl)-1-(4-methylphenyl)-1,5-dihydro-2H-pyrrol-2-one (14).** Started from 3-methylbenzaldehyde **1i** (600 mg, 5.00 mmol, 1.00 eq.), 4-methylaniline **2b** (536 mg, 5.00 mmol, 1.00 eq.) and ethyl 2,4-dioxopentanoate **3a** (627  $\mu$ L, 5.00 mmol, 1.00 eq.) in 12 mL of acetic acid. Yield: 560 mg, 35%, white solid. <sup>1</sup>H NMR (400 MHz, DMSO-*d*<sub>6</sub>):  $\delta$  7.43 (d, *J* = 8.4 Hz, 2H), 7.11-7.05 (m, 3H), 7.02 (d, *J* = 8.4 Hz, 2H), 6.93 (d, *J* = 7.2 Hz, 1H), 5.94 (s, 1H), 2.31 (s, 3H), 2.19 (s, 3H), 2.18 (s, 3H) ppm. MS [ESI+H]<sup>+</sup>: 321.93

**4-Acetyl-3-hydroxy-5-(3-methoxyphenyl)-1-(4-methylphenyl)-1,5-dihydro-2H-pyrrol-2-one (15).** Started from 3-methoxybenzaldehyde **1j** (681 mg, 5.00 mmol, 1.00 eq.), 4-methylaniline **2b** (536 mg, 5.00 mmol, 1.00 eq.) and ethyl 2,4-dioxopentanoate **3a** (627  $\mu$ L, 5.00 mmol, 1.00 eq.) in 12 mL of acetic acid. Yield: 1.27 g, 75%, white solid. <sup>1</sup>H NMR (400 MHz, DMSO-*d*<sub>6</sub>):  $\delta$  7.44 (d, *J* = 8.4 Hz, 2H), 7.12 - 7.07 (m, 3H), 6.79 (s, 1H), 6.75 (d, *J* = 0.8 Hz, 1H), 6.69 (dd, *J* = 8.0, 2.2 Hz, 1H), 5.97 (s, 1H), 3.65 (s, 3H), 2.32 (s, 3H), 2.20 (s, 3H) ppm. MS [ESI+H]<sup>+</sup>: 337.39.

**4-Acetyl-5-(3-chlorophenyl)-3-hydroxy-1-(4-methylphenyl)-1,5-dihydro-2H-pyrrol-2-one (16).** Started from 3-chlorobenzaldehyde **1k** (703 mg, 5.00 mmol, 1.00 eq.), 4-methylaniline **2b** (536 mg, 5.00 mmol, 1.00 eq.) and ethyl 2,4-dioxopentanoate **3a** (627  $\mu$ L, 5.00 mmol, 1.00 eq.) in 12 mL of acetic acid. Yield: 619 mg, 36%, light yellow solid. <sup>1</sup>H NMR (400 MHz, CDCl<sub>3</sub>):  $\delta$  7.28 (d, *J* = 8.4 Hz, 2H), 7.21-7.18 (m, 3H), 7.17-7.13 (m, 1H), 7.10 (d, *J* = 8.4 Hz, 2H), 5.75 (s, 1H), 2.29 (s, 3H), 2.27 (s, 3H) ppm. MS [ESI+H]<sup>+</sup>: 341.80

**4-Acetyl-5-(3-bromophenyl)-3-hydroxy-1-(4-methylphenyl)-1,5-dihydro-2H-pyrrol-2-one (17).** Started from 3-bromobenzaldehyde **1l** (925 mg, 5.00 mmol, 1.00 eq.), 4-methylaniline **2b** (536 mg, 5.00 mmol, 1.00 eq.) and ethyl 2,4-dioxopentanoate **3a** (627  $\mu$ L, 5.00 mmol, 1.00 eq.) in 12 mL of acetic acid. Yield: 993 mg, 51%, brown solid. <sup>1</sup>H NMR (400 MHz, DMSO-*d*<sub>6</sub>):  $\delta$  7.48 (t, *J* = 1.6 Hz, 1H), 7.44 (d, *J* = 8.4 Hz, 2H), 7.34-7.30 (m, 1H), 7.20 (dt, *J* = 8.0, 1.6 Hz, 1H), 7.14 (t, *J* = 7.6 Hz, 1H), 7.10 (d, *J* = 8.4 Hz, 2H), 6.02 (s, 1H), 2.33 (s, 3H), 2.20 (s, 3H) ppm. MS [ESI+H]<sup>+</sup>: 386.67

**5-Cyclohexyl-3-hydroxy-4-propionyl-1-(4-methylphenyl)-1,5-dihydro-2H-pyrrol-2-one (18).** Started from cyclohexane carboxaldehyde **1a** (129 mg, 1.15 mmol, 1.00 eq.), 4-methylaniline **2b** (123 mg, 1.15 mmol, 1.00 eq.) and ethyl 2,4-dioxohexanoate<sup>50</sup> **3b** (198 mg, 1.15 mmol, 1.00 eq.) in 3 mL of acetic acid. Yield: 65 mg, 19%, white solid. <sup>1</sup>H NMR (400 MHz, CDCl<sub>3</sub>):  $\delta$  7.31-7.23 (m, 4H), 4.96 (s, 1H), 2.95-2.82 (m, 2H), 2.38 (s, 3H), 1.90 (t, *J* = 10.8 Hz, 1H), 1.66-1.54 (m, 4H), 1.43-1.41 (m, 1H), 1.17 (t, *J* = 7.2 Hz, 3H), 1.09-1.03 (m, 3H), 0.98-0.86 (m, 1H), 0.71-0.61 (m, 1H) ppm. MS [ESI+H]<sup>+</sup>: 328.13.

**4-Butyryl-5-cyclohexyl-3-hydroxy-1-(4-methylphenyl)-1,5-dihydro-2H-pyrrol-2-one (19).**<sup>32</sup> Started from cyclohexane carboxaldehyde **1a** (605  $\mu$ L, 5.00 mmol, 1.00 eq.), 4-methylaniline **2b** (536 mg, 5.00 mmol, 1.00 eq.) and ethyl 2,4-dioxoheptanoate<sup>34</sup> **3c** (198 mg, 1.15 mmol, 1.00 eq.) in 12 mL of acetic acid. Yield: 669 mg (39%) as a white solid. <sup>1</sup>H NMR (400 MHz, DMSO):  $\delta$  7.39 (d, *J* = 8.4 Hz, 2H), 7.24 (d, *J* = 8.0 Hz, 2H), 5.02 (s, 1H), 2.89-2.70 (m, 2H), 2.32 (s, 3H), 1.84-1.78 (m, 1H), 1.61-1.32 (m, 7H), 0.97-0.80 (m, 6H), 0.80-0.73 (m, 1H), 0.57-0.48 (m, 1H) ppm. MS [ESI+H]<sup>+</sup>: 341.87.



**4-Pentanoyl-5-cyclohexyl-3-hydroxy-1-(4-methylphenyl)-1,5-dihydro-2H-pyrrol-2-one (20).**

Started from cyclohexane carboxaldehyde **1a** (266 mg, 2.37 mmol, 1.00 eq.), 4-methylaniline **2b** (253 mg, 2.37 mmol, 1.00 eq.) and ethyl 2,4-dioxooctanoate<sup>34</sup> **3d** (475 mg, 2.37 mmol, 1.00 eq.) in 5 mL of acetic acid. Yield: 237 mg, 28%, white solid. <sup>1</sup>H NMR (400 MHz, DMSO): δ 12.02 (br s, 1H), 7.39 (d, *J* = 8.0 Hz, 2H), 7.24 (d, *J* = 7.6 Hz, 2H), 5.02 (s, 1H), 2.92-2.73 (m, 2H), 2.32 (s, 3H), 1.85-1.75 (m, 1H), 1.58-1.28 (m, 9H), 0.91-0.65 (m, 7H) 0.57-0.50 (m, 1H) ppm. MS [ESI+H]<sup>+</sup>: 356.00.

**5-Cyclohexyl-3-hydroxy-4-isobutyryl-1-(4-methylphenyl)-1,5-dihydro-2H-pyrrol-2-one (21).**

Started from cyclohexane carboxaldehyde **1a** (535 μL, 4.42 mmol, 1.00 eq.), 4-methylaniline **2b** (474 mg, 4.42 mmol, 1.00 eq.) and ethyl 2,4-dioxo-5-methylhexanoate **3e** (823 mg, 4.42 mmol, 1.00 eq.) in 10 mL of acetic acid. Yield: 255 mg, 17%, white solid. <sup>1</sup>H NMR (400 MHz, DMSO-*d*<sub>6</sub>): δ 12.07 (br s, 1H), 7.40 (d, *J* = 7.6 Hz, 2H), 7.24 (d, *J* = 7.6 Hz, 2H), 5.03 (d, *J* = 1.6 Hz, 1H), 3.44-3.41 (m, 1H), 2.32 (s, 3H), 1.80-1.70 (m, 1H), 1.62-1.59 (m, 1H), 1.46-1.37 (m, 4H), 1.09 (d, *J* = 6.8 Hz, 3H), 1.02 (d, *J* = 6.8 Hz, 3H), 0.97-0.77 (m, 4H), 0.59-0.53 (m, 1H) ppm. MS [ESI+H]<sup>+</sup>: 342.13.

**5-Cyclohexyl-4-(cyclopropanecarbonyl)-3-hydroxy-1-(4-methylphenyl)-1,5-dihydro-2H-pyrrol-2-one (22).** Started from cyclohexane carboxaldehyde **1a** (605 μL, 5.00 mmol, 1.00 eq.), 4-methylaniline **2b** (550 μL, 5.00 mmol, 1.00 eq.) and ethyl 4-cyclopropyl-2,4-dioxobutanoate<sup>51</sup> **3f** (920 mg, 5.00 mmol, 1.00 eq.) in 10 mL of AcOH. Yield: 60 mg, 4%, white solid. <sup>1</sup>H NMR (400 MHz, MeOD): δ 7.34 (d, *J* = 8.4 Hz, 2H), 7.27 (d, *J* = 7.6 Hz, 2H), 5.01 (d, *J* = 2.0 Hz, 1H), 3.01-2.95 (m, 1H), 2.38 (s, 3H), 1.88 (t, *J* = 10.4 Hz, 1H), 1.72-1.64 (m, 1H), 1.60-1.48 (m, 3H), 1.41 (d, *J* = 11.2 Hz, 1H), 1.04-0.86 (m, 8H), 0.72-0.62 (m, 1H) ppm. MS [ESI+Na]<sup>+</sup>: 363.10.

**5-Cyclohexyl-3-hydroxy-1-(4-methylphenyl)-4-pivaloyl-1,5-dihydro-2H-pyrrol-2-one (23).<sup>32</sup>**

Started from cyclohexane carboxaldehyde **1a** (121 μL, 1.00 mmol, 1.00 eq.), 4-methylaniline **2b** (107 mg, 1.00 mmol, 1.00 eq.) and ethyl 5,5-dimethyl-2,4-dioxohexanoate **3g** (175 μL, 1.00 mmol, 1.00 eq.) in 3 mL of acetic acid. Yield: 20 mg, 6%, white solid. <sup>1</sup>H NMR (400 MHz, DMSO-*d*<sub>6</sub>): δ 7.41 (d, *J* = 8.4 Hz, 2H), 7.25 (d, *J* = 8.4 Hz, 2H), 5.11 (d, *J* = 2.2 Hz, 1H), 2.32 (s, 3H), 1.63-1.58 (m, 2H), 1.52-1.46 (m, 3H), 1.31-1.28 (m, 1H) 1.25 (s, 9H) 1.01-0.69 (m, 4H), 0.69-0.59 (m, 1H) ppm. MS [ESI+H]<sup>+</sup>: 356.13.

**Ethyl 2-cyclohexyl-4-hydroxy-5-oxo-1-(4-methylphenyl)-2,5-dihydro-1H-pyrrole-3-carboxylate (24).**<sup>29</sup> Sodium 1,4-diethoxy-1,4-dioxobut-2-en-2-olate (1.25 g, 6.00 mmol) was dissolved in 25 mL H<sub>2</sub>O and 25 mL Et<sub>2</sub>O was added. Acidified to pH 2 with 6M HCl (aq.) and was extracted with Et<sub>2</sub>O from the aqueous phase, dried over MgSO<sub>4</sub> and concentrated *in vacuo* yielding 1.05 g, 4.97 mmol, 83% diethyl 2-oxosuccinate as a yellow oil.<sup>52</sup> Diethyl 2-oxosuccinate **3h** (1.05 g, 4.97 mmol, 1.12 eq.) was added to a mixture of cyclohexane carboxaldehyde **1a** (534 μL, 4.42 mmol, 1.00 eq.) and 4-methylaniline **2b** (474 mg, 4.42 mmol, 1.00 eq.) in 10 mL of dry THF and stirred at room temperature overnight. The reaction mixture was concentrated *in vacuo*, Et<sub>2</sub>O was added and the white precipitate was collected by filtration. Yield: 400 mg, 26%, white solid. <sup>1</sup>H NMR (400 MHz, CDCl<sub>3</sub>): δ 11.24 (s, 1H), 7.40 (d, *J* = 8.4 Hz, 2H), 7.24 (d, *J* = 8.4 Hz, 2H), 5.00 (d, *J* = 1.8 Hz, 1H), 4.32-4.13 (m, 2H), 2.32 (s, 3H), 1.85-1.76 (m, 1H), 1.66-1.59 (m, 1H), 1.56-1.44 (m, 3H), 1.32 (d, *J* = 12.0 Hz, 1H), 1.26 (t, *J* = 7.2 Hz, 3H), 1.06-0.75 (m, 4H), 0.63-0.53 (m, 1H) ppm. MS [ESI+H]<sup>+</sup>: 344.07.

**Isopropyl 2-cyclohexyl-4-hydroxy-5-oxo-1-(4-methylphenyl)-2,5-dihydro-1H-pyrrole-3-carboxylate (25).** Ester **22** (343 mg, 1.00 mmol, 1.00 eq.) and *p*-toluenesulfonic acid (172 mg, 1.00 mmol, 1.00 eq.) were dissolved in 10 mL of 2-propanol and the reaction mixture was refluxed for 48 hours. The solvent was removed under reduced pressure, the crude product was dissolved in 50 mL EtOAc and washed 3x with H<sub>2</sub>O, dried over MgSO<sub>4</sub>, filtered and concentrated under reduced pressure. The crude product was purified by column chromatography (4/1 EtOAc/Pet ether) and yielded 150 mg, 9.5%, brownish solid. <sup>1</sup>H NMR (400 MHz, CDCl<sub>3</sub>): δ 9.33 (s, 1H), 7.30 (d, *J* = 8.4 Hz, 2H), 7.22 (d, *J* = 8.4 Hz, 2H), 5.31-5.23 (m, 1H), 4.79 (d, *J* = 2.0 Hz, 1H), 2.37 (s, 3H), 1.88 (td, *J* = 9.6, 2.8 Hz, 1H), 1.73-1.66 (m, 1H), 1.63-1.50 (m, 3H), 1.38 (d, *J* = 6.8 Hz, 6H), 1.29-1.19 (m, 1H), 1.13-0.90 (m, 4H), 0.74-0.64 (m, 1H) ppm. MS [ESI+H]<sup>+</sup>: 357.93.

**4-Benzoyl-5-cyclohexyl-3-hydroxy-1-(4-methylphenyl)-1,5-dihydro-2H-pyrrol-2-one (26).** Started from cyclohexane carboxaldehyde **1a** (484  $\mu$ L, 4.00 mmol, 1.00 eq.), 4-methylaniline **2b** (428 mg, 4.00 mmol, 1.00 eq.) and ethyl 2,4-dioxo-4-phenylbutanoate<sup>53</sup> **3i** (880 mg, 4.00 mmol, 1.00 eq.) in 10 mL of AcOH. Yield: 53 mg, 4%, white solid. <sup>1</sup>H NMR (400 MHz, DMSO-*d*<sub>6</sub>):  $\delta$  7.85 (d, *J* = 7.6 Hz, 2H), 7.69-7.62 (m, 1H), 7.58-7.52 (m, 2H), 7.49 (d, *J* = 8.0 Hz, 2H), 7.29 (d, *J* = 8.4 Hz, 2H), 5.32 (s, 1H), 2.35 (s, 3H), 1.73-1.62 (m, 2H), 1.58-1.51 (m, 2H), 1.49-1.37 (m, 2H), 1.05-0.94 (m, 1H), 0.88-0.74 (m, 4H) ppm. MS [ESI+H]<sup>+</sup>: 375.93.

**4-Acetyl-5-cyclohexyl-3-hydroxy-1-phenyl-1,5-dihydro-2H-pyrrol-2-one (27).**<sup>32</sup> Started from cyclohexane carboxaldehyde **1a** (534  $\mu$ L, 4.42 mmol, 1.00 eq.), aniline **2a** (400  $\mu$ L, 4.42 mmol, 1.00 eq.) and ethyl 2,4-dioxopentanoate **3a** (554  $\mu$ L, 4.42 mmol, 1.00 eq.) in 10 mL of AcOH. Yield: 1.00 g, 76%, yellow solid. <sup>1</sup>H NMR (400 MHz, CDCl<sub>3</sub>):  $\delta$  7.47-7.44 (m, 4H), 7.32-7.28 (m, 1H), 4.99 (d, *J* = 2.0 Hz, 1H), 2.54 (s, 3H), 1.97-1.90 (m, 1H), 1.69-1.66 (m, 1H), 1.59-1.48 (m, 3H), 1.45-1.41 (m, 1H), 1.10-0.99 (m, 3H), 0.92-0.86 (m, 1H), 0.63 (qd, *J* = 9.2, 3.6 Hz, 1H) ppm. MS [ESI+H]<sup>+</sup>: 300.07

**4-Acetyl-5-cyclohexyl-1-(4-ethylphenyl)-3-hydroxy-1,5-dihydro-2H-pyrrol-2-one (28).**<sup>32</sup> Started from cyclohexane carboxaldehyde **1a** (534  $\mu$ L, 4.42 mmol, 1.00 eq.), 4-ethylaniline **2c** (553  $\mu$ L, 4.42 mmol, 1.00 eq.) and ethyl 2,4-dioxopentanoate **3a** (554  $\mu$ L, 4.42 mmol, 1.00 eq.) in 10 mL of AcOH. Yield: 134 mg, 9%, light-yellow solid. <sup>1</sup>H NMR (400 MHz, CDCl<sub>3</sub>):  $\delta$  7.32 (d, *J* = 8.4 Hz, 2H), 7.25 (d, *J* = 6.4 Hz, 2H), 4.94 (s, 1H), 2.68 (q, *J* = 7.6 Hz, 2H), 2.54 (s, 3H), 1.95-1.90 (m, 1H), 1.68-1.66 (m, 1H), 1.67-1.51 (m, 3H), 1.43-1.41 (m, 1H), 1.26 (t, *J* = 7.6 Hz, 3H), 1.10-0.98 (m, 4H), 0.90-0.87 (m, 1H), 0.69-0.60 (m, 1H) ppm. MS [ESI+H]<sup>+</sup>: 328.13

**4-Acetyl-5-cyclohexyl-3-hydroxy-1-(4-methoxyphenyl)-1,5-dihydro-2H-pyrrol-2-one (29).**<sup>32</sup> Started from cyclohexane carboxaldehyde **1a** (534  $\mu$ L, 4.42 mmol, 1.00 eq.), 4-methoxyaniline **2d** (560 mg, 4.42 mmol, 1.00 eq.) and ethyl 2,4-dioxopentanoate **3a** (554  $\mu$ L, 4.42 mmol, 1.00 eq.) in 10 mL of AcOH. Yield: 805 mg, 56%, light-yellow solid. <sup>1</sup>H NMR (400 MHz, DMSO-*d*<sub>6</sub>):  $\delta$  7.41 (d, *J* = 8.8 Hz, 2H), 7.00 (d, *J* = 9.2 Hz, 2H), 4.96 (d, *J* = 1.2 Hz, 1H), 3.77 (s, 3H), 2.43 (s, 3H), 1.86-1.80 (m, 1H), 1.60-1.58 (m, 1H), 1.40-1.37 (m, 2H), 1.35-1.32 (m, 2H), 0.99-0.91 (m, 3H), 0.87-0.75 (m, 1H), 0.58-0.55 (m, 1H) ppm. MS [ESI+H]<sup>+</sup>: 330.07

**4-Acetyl-1-(4-chlorophenyl)-5-cyclohexyl-3-hydroxy-1,5-dihydro-2H-pyrrol-2-one (30).**<sup>32</sup> Started from cyclohexane carboxaldehyde **1a** (534  $\mu$ L, 4.42 mmol, 1.00 eq.), 4-chloroaniline **2e** (544 mg, 4.42 mmol, 1.00 eq.) and ethyl 2,4-dioxopentanoate **3a** (554  $\mu$ L, 4.42 mmol, 1.00 eq.) in 10 mL of AcOH. Yield: 713 mg, 48%, light-yellow solid. <sup>1</sup>H NMR (400 MHz, CDCl<sub>3</sub>):  $\delta$  8.75 (s br, 1H), 7.42 (d, *J* = 8.8 Hz, 2H), 7.39 (d, *J* = 9.2 Hz, 2H), 4.95 (d, *J* = 2.0 Hz, 1H), 2.53 (s, 3H), 1.96-1.84 (m, 1H), 1.75-1.65 (m, 1H), 1.63-1.51 (m, 3H), 1.45-1.40 (m, 1H), 1.11-0.97 (m, 3H), 0.95-0.86 (m, 1H), 0.66 (qd, *J* = 12.4, 3.2 Hz, 1H) ppm. MS [ESI+H]<sup>+</sup>: 334.1

**4-Acetyl-1-(4-bromophenyl)-5-cyclohexyl-3-hydroxy-1,5-dihydro-2H-pyrrol-2-one (31).**<sup>32</sup> Started from cyclohexane carboxaldehyde **1a** (534  $\mu$ L, 4.42 mmol, 1.00 eq.), 4-bromoaniline **2f** (760 mg, 4.42 mmol, 1.00 eq.) and ethyl 2,4-dioxopentanoate **3a** (554  $\mu$ L, 4.42 mmol, 1.00 eq.) in 10 mL of AcOH. Yield: 910 mg, 53%, white solid. <sup>1</sup>H NMR (400 MHz, CDCl<sub>3</sub>):  $\delta$  7.57 (d, *J* = 8.4 Hz, 2H), 7.33 (d, *J* = 8.4 Hz, 2H), 4.96 (s, 1H), 2.53 (s, 3H), 1.97-1.87 (m, 1H), 1.73-1.65 (m, 1H), 1.62-1.49 (m, 3H), 1.45-1.37 (m, 1H), 1.15-0.97 (m, H), 0.95-0.86 (m, 1H), 0.66 (qd, *J* = 12.4, 3.2 Hz, 1H) ppm. MS [ESI+H]<sup>+</sup>: 378.1

**4-Acetyl-5-cyclohexyl-3-hydroxy-1-(4-(trifluoromethyl)phenyl)-1,5-dihydro-2H-pyrrol-2-one (32).**<sup>32</sup> Started from cyclohexane carboxaldehyde **1a** (534  $\mu$ L, 4.42 mmol, 1.00 eq.), 4-trifluoromethylaniline **2g** (556  $\mu$ L, 4.42 mmol, 1.00 eq.) and ethyl 2,4-dioxopentanoate **3a** (554  $\mu$ L, 4.42 mmol, 1.00 eq.) in 10 mL of AcOH. Yield: 80 mg, 5%, white solid. <sup>1</sup>H NMR (400 MHz, DMSO-*d*<sub>6</sub>):  $\delta$  12.25 (s, 1H), 7.82 (s, 4H), 5.19 (s, 1H), 2.46 (s, 3H), 1.85 (t, *J* = 11.2 Hz, 1H), 1.60 (d, *J* = 10.8 Hz, 1H), 1.54-1.43 (m, 3H), 1.38 (d, *J* = 12.4 Hz, 1H), 1.05-0.74 (m, 4H), 0.52 (d, *J* = 12.4 Hz, 1H) ppm. MS [ESI+H]<sup>+</sup>: 369.07

**4-Acetyl-5-cyclohexyl-3-hydroxy-1-(3-methylphenyl)-1,5-dihydro-2H-pyrrol-2-one (33).**<sup>29</sup> Started from cyclohexane carboxaldehyde **1a** (534  $\mu$ L, 4.42 mmol, 1.00 eq.), 3-methylaniline **2h** (474

$\mu\text{L}$ , 4.42 mmol, 1.00 eq.) and ethyl 2,4-dioxopentanoate **3a** (554  $\mu\text{L}$ , 4.42 mmol, 1.00 eq.) in 10 mL of AcOH. Yield: 511 mg, 37%, white solid.  $^1\text{H NMR}$  (400 MHz,  $\text{CDCl}_3$ ):  $\delta$  7.32 (t,  $J = 8.0$  Hz, 1H), 7.26 (s, 1H), 7.19 (d,  $J = 8.0$  Hz, 1H), 7.11 (d,  $J = 7.6$  Hz, 1H), 4.96 (d,  $J = 2.0$  Hz, 1H), 2.53 (s, 3H), 2.40 (s, 3H), 1.95-1.88 (m, 1H), 1.69-1.65 (m, 1H), 1.59-1.50 (m, 3H), 1.45-1.39 (m, 1H), 1.15-0.84 (m, 4H), 0.64 (qd,  $J = 12.4$ , 3.6 Hz, 1H) ppm. MS [ESI+H] $^+$ : 314.07

**4-Acetyl-5-cyclohexyl-1-(3-fluorophenyl)-3-hydroxy-1,5-dihydro-2H-pyrrol-2-one (34).**<sup>32</sup>

Started from cyclohexane carboxaldehyde **1a** (534  $\mu\text{L}$ , 4.42 mmol, 1.00 eq.), 3-fluoroaniline **2i** (425  $\mu\text{L}$ , 4.42 mmol, 1.00 eq.) and ethyl 2,4-dioxopentanoate **3a** (554  $\mu\text{L}$ , 4.42 mmol, 1.00 eq.) in 10 mL of AcOH. Yield: 226 mg, 16%, white solid.  $^1\text{H NMR}$  (400 MHz,  $\text{CDCl}_3$ ):  $\delta$  8.99 (s br, 1H), 7.45-7.34 (m, 1H), 7.29-7.25 (m, 1H), 7.21 (d,  $J = 8.0$  Hz, 1H), 7.01 (td,  $J = 8.0$ , 2.0 Hz, 1H), 4.97 (d,  $J = 2.0$  Hz, 1H), 2.55 (s, 3H), 1.94 (td,  $J = 12.0$ , 2.0 Hz, 1H), 1.70-1.67 (m, 1H), 1.62-1.53 (m, 3H), 1.47-1.40 (m, 1H), 1.15-0.97 (m, 3H), 0.96-0.84 (m, 1H), 0.66 (qd,  $J = 12.4$ , 3.6 Hz, 1H) ppm. MS [ESI+H] $^+$ : 318.27

**4-Acetyl-1-(3-chlorophenyl)-5-cyclohexyl-3-hydroxy-1,5-dihydro-2H-pyrrol-2-one (35).**<sup>29</sup>

Started from cyclohexane carboxaldehyde **1a** (534  $\mu\text{L}$ , 4.42 mmol, 1.00 eq.), 3-chloroaniline **2j** (468  $\mu\text{L}$ , 4.42 mmol, 1.00 eq.) and ethyl 2,4-dioxopentanoate **3a** (554  $\mu\text{L}$ , 4.42 mmol, 1.00 eq.) in 10 mL of AcOH. Yield: 805 mg, 55%, yellow solid.  $^1\text{H NMR}$  (400 MHz,  $\text{CDCl}_3$ ):  $\delta$  8.92 (s br, 1H), 7.51 (t,  $J = 1.6$  Hz, 1H), 7.38 (t,  $J = 8.0$  Hz, 1H), 7.32 (d,  $J = 8.0$  Hz, 1H), 7.29-7.25 (m, 1H), 4.96 (d,  $J = 2.0$  Hz, 1H), 2.55 (s, 3H), 1.93 (td,  $J = 12.4$ , 2.0 Hz, 1H), 1.71-1.68 (m, 1H), 1.60-1.54 (m, 3H), 1.46-1.43 (m, 1H), 1.15-0.99 (m, 3H), 0.98-0.86 (m, 1H), 0.65 (qd,  $J = 12.4$ , 2.8 Hz, 1H) ppm. MS [ESI+H] $^+$ : 334.13

**4-Acetyl-5-cyclohexyl-3-hydroxy-1-(3-(trifluoromethyl)phenyl)-1,5-dihydro-2H-pyrrol-2-one (36).**

Started from cyclohexane carboxaldehyde **1a** (534  $\mu\text{L}$ , 4.42 mmol, 1.00 eq.), 3-trifluoromethylaniline **2k** (552  $\mu\text{L}$ , 4.42 mmol, 1.00 eq.) and ethyl 2,4-dioxopentanoate **3a** (554  $\mu\text{L}$ , 4.42 mmol, 1.00 eq.) in 10 mL of AcOH. Yield: 560 mg, 34%, brown solid.  $^1\text{H NMR}$  (400 MHz,  $\text{DMSO}-d_6$ ):  $\delta$  12.26 (br s, 1H), 7.98 (s, 1H), 7.86 (d,  $J = 7.6$  Hz, 1H), 7.69 (t,  $J = 8.0$  Hz, 1H), 7.64 (d,  $J = 7.6$  Hz, 1H), 5.23 (d,  $J = 1.2$  Hz, 1H), 2.45 (s, 3H), 1.86 (t,  $J = 11.2$  Hz, 1H), 1.62-1.58 (m, 1H), 1.47-1.35 (m, 4H), 1.00-0.85 (m, 3H), 0.80-0.71 (m, 1H), 0.47 (qd,  $J = 12.8$  Hz, 3.2 Hz, 1H) ppm. MS [ESI+H] $^+$ : 368.13

**4-Acetyl-5-cyclohexyl-1-(2-fluoro-4-methylphenyl)-3-hydroxy-1,5-dihydro-2H-pyrrol-2-one (37).**<sup>29</sup>

Started from cyclohexane carboxaldehyde **1a** (534  $\mu\text{L}$ , 4.42 mmol, 1.00 eq.), 2-fluoro-4-methylaniline **2l** (499  $\mu\text{L}$ , 4.42 mmol, 1.00 eq.) and ethyl 2,4-dioxopentanoate **3a** (554  $\mu\text{L}$ , 4.42 mmol, 1.00 eq.) in 10 mL of AcOH. Yield: 508 mg, 35%, white solid.  $^1\text{H NMR}$  (400 MHz,  $\text{CDCl}_3$ ):  $\delta$  9.35 (br s, 1H), 7.28-7.22 (m, 1H), 7.04-6.98 (m, 2H), 4.93 (d,  $J = 1.6$  Hz, 1H), 2.52 (s, 3H), 2.39 (s, 3H), 1.98-1.91 (m, 1H), 1.69-1.63 (m, 1H), 1.57-1.41 (m, 4H), 1.13-1.02 (m, 3H), 0.92-0.82 (m, 1H), 0.62 (qd,  $J = 12.8$  Hz, 3.2 Hz, 1H) ppm. MS [ESI+H] $^+$ : 332.1

**4-Acetyl-1-(4-chloro-2-fluorophenyl)-5-cyclohexyl-3-hydroxy-1,5-dihydro-2H-pyrrol-2-one (38).**<sup>29</sup>

Started from cyclohexane carboxaldehyde **1a** (534  $\mu\text{L}$ , 4.42 mmol, 1.00 eq.), 4-chloro-2-fluoroaniline **2m** (490  $\mu\text{L}$ , 4.42 mmol, 1.00 eq.) and ethyl 2,4-dioxopentanoate **3a** (554  $\mu\text{L}$ , 4.42 mmol, 1.00 eq.) in 10 mL of AcOH. Yield: 190 mg, 12%, light yellow solid.  $^1\text{H NMR}$  (400 MHz,  $\text{CDCl}_3$ ):  $\delta$  9.07 (br s, 1H), 7.37 (t,  $J = 8.4$  Hz, 1H), 7.28-7.22 (m, 2H), 4.96 (d,  $J = 2.0$  Hz, 1H), 2.52 (s, 3H), 2.00-1.91 (m, 1H), 1.72-1.65 (m, 1H), 1.63-1.44 (m, 4H), 1.14-1.00 (m, 2H), 0.99-0.82 (m, 2H), 0.61 (qd,  $J = 12.8$  Hz, 3.6 Hz, 1H) ppm. MS [ESI+H] $^+$ : 352.1

**4-Acetyl-1-(4-bromo-2-fluorophenyl)-5-cyclohexyl-3-hydroxy-1,5-dihydro-2H-pyrrol-2-one (39).**<sup>32</sup>

Started from cyclohexane carboxaldehyde **1a** (303  $\mu\text{L}$ , 2.50 mmol, 1.00 eq.), 4-bromo-2-fluoroaniline **2n** (475  $\mu\text{L}$ , 2.50 mmol, 1.00 eq.) and ethyl 2,4-dioxopentanoate **3a** (395  $\mu\text{L}$ , 2.50 mmol, 1.00 eq.) in 5 mL of AcOH. Purified by silica column chromatography using EtOAc/Pet Ether (1/6). The resulting impure product was stirred in diisopropylether and the pure product was obtained by filtration. Yield: 36 mg, 4%, white solid.  $^1\text{H NMR}$  (400 MHz,  $\text{CDCl}_3$ ):  $\delta$  8.97 (s br, 1H, OH), 7.43-7.36 (m, 2H), 7.31 (t,  $J = 8.0$  Hz, 1H), 4.96 (d,  $J = 1.2$  Hz, 1H), 2.52 (s, 3H), 1.94 (t,  $J = 11.6$  Hz, 1H), 1.68 (d,  $J = 13.2$  Hz, 1H), 1.57-1.42 (m, 4H), 1.15-0.84 (m, 4H), 0.62 (qd,  $J = 12.4$ , 3.2 Hz, 1H) ppm. MS [ESI+H] $^+$ : 395.67

**4-Acetyl-5-cyclohexyl-1-(3,4-dimethylphenyl)-3-hydroxy-1,5-dihydro-2H-pyrrol-2-one (40).**<sup>32</sup> Started from cyclohexane carboxaldehyde **1a** (303  $\mu$ L, 2.50 mmol, 1.00 eq.), 3,4-dimethylaniline **2o** (303  $\mu$ L, 2.50 mmol, 1.00 eq.) and ethyl 2,4-dioxopentanoate **3a** (395  $\mu$ L, 2.50 mmol, 1.00 eq.) in 5 mL of AcOH. Yield: 167 mg, 20%, white solid. <sup>1</sup>H NMR (400 MHz, CDCl<sub>3</sub>):  $\delta$  9.06 (s br, 1H, OH), 7.21-7.16 (m, 2H), 7.10 (dd,  $J$  = 8.0, 1.6 Hz, 1H), 4.92 (d,  $J$  = 2.0 Hz, 1H), 2.53 (s, 3H), 2.29 (s, 3H), 2.28 (s, 3H), 1.92 (t,  $J$  = 11.6 Hz, 1H), 1.73-1.65 (m, 1H), 1.60-1.49 (m, 3H), 1.42 (d,  $J$  = 12.4 Hz, 1H), 1.13-0.98 (m, 3H), 0.94-0.84 (m, 1H), 0.65 (qd,  $J$  = 12.0, 3.2 Hz, 1H) ppm. MS [ESI+H]<sup>+</sup>: 327.87

**4-Acetyl-1-(4-chloro-3-methylphenyl)-5-cyclohexyl-3-hydroxy-1,5-dihydro-2H-pyrrol-2-one (41).**<sup>29</sup> Started from cyclohexane carboxaldehyde **1a** (534  $\mu$ L, 4.42 mmol, 1.00 eq.), 4-chloro-3-methylaniline **2p** (626 mg, 4.42 mmol, 1.00 eq.) and ethyl 2,4-dioxopentanoate **3a** (554  $\mu$ L, 4.42 mmol, 1.00 eq.) in 10 mL of AcOH. Yield: 505 mg, 33%, white solid. <sup>1</sup>H NMR (400 MHz, CDCl<sub>3</sub>):  $\delta$  9.39 (s br, 1H, OH), 7.40 (d,  $J$  = 8.4 Hz, 1H), 7.32 (d,  $J$  = 2.0 Hz, 1H), 7.17 (dd,  $J$  = 8.4, 2.4 Hz, 1H), 4.94 (d,  $J$  = 2.0 Hz, 1H), 2.55 (s, 3H), 2.42 (s, 3H), 1.93 (td,  $J$  = 12.0, 2.4 Hz, 1H), 1.72-1.64 (m, 1H), 1.60-1.49 (m, 3H), 1.46-1.34 (m, 1H), 1.15-0.96 (m, 3H), 0.94-0.84 (m, 1H), 0.65 (qd,  $J$  = 12.8, 3.6 Hz, 1H) ppm. MS [ESI+H]<sup>+</sup>: 348.0

**4-Acetyl-5-cyclohexyl-1-(3-fluoro-4-methylphenyl)-3-hydroxy-1,5-dihydro-2H-pyrrol-2-one (42).**<sup>32</sup> Started from cyclohexane carboxaldehyde **1a** (534  $\mu$ L, 4.42 mmol, 1.00 eq.), 3-fluoro-4-methylaniline **2q** (506  $\mu$ L, 4.42 mmol, 1.00 eq.) and ethyl 2,4-dioxopentanoate **3a** (554  $\mu$ L, 4.42 mmol, 1.00 eq.) in 10 mL of AcOH. Yield: 160 mg, 10%, white solid. <sup>1</sup>H NMR (400 MHz, CDCl<sub>3</sub>):  $\delta$  7.24 (t,  $J$  = 8.0 Hz, 1H), 7.18 (dd,  $J$  = 6.8, 2.0 Hz, 1H), 7.09 (dd,  $J$  = 8.4, 2.0 Hz, 1H), 4.92 (d,  $J$  = 2.0 Hz, 1H), 2.54 (s, 3H), 2.30 (d,  $J$  = 1.6 Hz, 3H), 1.94 (td,  $J$  = 12.0, 2.0 Hz, 1H), 1.74-1.64 (m, 1H), 1.64-1.48 (m, 3H), 1.48-1.39 (m, 1H), 1.14-0.98 (m, 3H), 0.98-0.84 (m, 1H), 0.67 (qd,  $J$  = 12.8, 3.2 Hz, 1H). MS [ESI+H]<sup>+</sup>: 332.00

**1-(4-Bromo-2-fluorophenyl)-5-cyclohexyl-4-(cyclopropanecarbonyl)-3-hydroxy-1,5-dihydro-2H-pyrrol-2-one (43).** Started from cyclohexane carboxaldehyde **1a** (242  $\mu$ L, 2.00 mmol, 1.00 eq.), 4-bromo-2-fluoroaniline **2n** (380 mg, 2.00 mmol, 1.00 eq.) and ethyl 4-cyclopropyl-2,4-dioxobutanoate<sup>51</sup> **3f** (368 mg, 2.00 mmol, 1.00 eq.) in 5 mL of AcOH. Yield: 240 mg, 28%, white solid. <sup>1</sup>H NMR (400 MHz, CDCl<sub>3</sub>):  $\delta$  7.43-7.34 (m, 3H), 5.06 (d,  $J$  = 1.6 Hz, 1H), 2.39-2.33 (m, 1H), 1.92 (t,  $J$  = 12.0 Hz, 1H), 1.72 (d,  $J$  = 12.4 Hz, 1H), 1.64-1.48 (m, 4H), 1.35-1.31 (m, 1H), 1.25-1.22 (m, 1H), 1.13-1.01 (m, 5H), 0.99-0.90 (m, 1H), 0.68 (qd,  $J$  = 12.4, 3.2 Hz, 1H) ppm. MS [ESI+H]<sup>+</sup>: 421.67

**4-Benzoyl-1-(4-bromo-2-fluorophenyl)-5-cyclohexyl-3-hydroxy-1,5-dihydro-2H-pyrrol-2-one (44).** Started from cyclohexane carboxaldehyde **1a** (242  $\mu$ L, 2.00 mmol, 1.00 eq.), 4-bromo-2-fluoroaniline **2n** (380 mg, 2.00 mmol, 1.00 eq.) and ethyl 2,4-dioxo-4-phenylbutanoate<sup>53</sup> **3i** (440 mg, 2.00 mmol, 1.00 eq.) in 5 mL of AcOH. Yield: 210 mg, 23%, white solid. <sup>1</sup>H NMR (400 MHz, DMSO):  $\delta$  7.84 (d,  $J$  = 6.8 Hz, 2H), 7.78 (dd,  $J$  = 10.4, 2.0 Hz, 1H), 7.67-7.60 (m, 2H), 7.58-7.51 (m, 3H), 5.21 (d,  $J$  = 2.0 Hz, 1H), 1.64-1.44 (m, 6H), 1.00-0.70 (m, 5H) ppm. MS [ESI+H]<sup>+</sup>: 459.87

**1-(4-Bromo-2-fluorophenyl)-5-(3-bromophenyl)-4-(cyclopropanecarbonyl)-3-hydroxy-1,5-dihydro-2H-pyrrol-2-one (45).** Started from 3-bromobenzaldehyde **1l** (233  $\mu$ L, 2.00 mmol, 1.00 eq.), 4-bromo-2-fluoroaniline **2n** (380 mg, 2.00 mmol, 1.00 eq.) and ethyl 4-cyclopropyl-2,4-dioxobutanoate<sup>51</sup> **3f** (440 mg, 2.00 mmol, 1.00 eq.) in 5 mL of AcOH. Yield: 205 mg, 21%, off-white solid. <sup>1</sup>H NMR (400 MHz, CDCl<sub>3</sub>):  $\delta$  7.40 (d,  $J$  = 6.8 Hz, 1H), 7.35-7.27 (m, 2H), 7.22 (d,  $J$  = 8.4 Hz, 1H), 7.19-7.11 (m, 2H), 7.07 (t,  $J$  = 8.0 Hz, 1H), 5.84 (s, 1H), 1.93-1.85 (m, 1H), 1.22-1.19 (m, 1H), 1.07-0.97 (m, 2H), 0.82-0.74 (m, 1H) ppm. MS [ESI+H]<sup>+</sup>: 495.67

**4-Acetyl-1-(4-bromo-2-fluorophenyl)-5-(3-bromophenyl)-3-hydroxy-1,5-dihydro-2H-pyrrol-2-one (46).** Started from 3-bromobenzaldehyde **1l** (291  $\mu$ L, 2.50 mmol, 1.00 eq.), 4-bromo-2-fluoroaniline **2n** (475 mg, 2.50 mmol, 1.00 eq.) and ethyl 2,4-dioxopentanoate **3a** (395 mg, 2.50 mmol, 1.00 eq.) in 5 mL of AcOH. Purified by silica column chromatography using EtOAc/Pet Ether (1/19). Yield: 82 mg, 5%, yellow solid. <sup>1</sup>H NMR (400 MHz, CDCl<sub>3</sub>):  $\delta$  7.41 (dt,  $J$  = 7.6, 1.6 Hz, 1H), 7.33-7.24 (m, 2H), 7.22 (d,  $J$  = 8.4 Hz, 1H), 7.19-7.11 (m, 2H), 7.08 (t,  $J$  = 8.0 Hz, 1H), 5.74 (s, 1H), 2.17 (s, 3H) ppm. MS [ESI+H]<sup>+</sup>: 469.60

## In vitro characterization of compound's activity

### Chemicals and reagents

[<sup>3</sup>H]-CCR2-RA-[R] (specific activity 59.6 Ci mmol<sup>-1</sup>), corresponding to the (*R*)-isomer of compound **38** ([<sup>3</sup>H]-(*R*)-4-acetyl-1-(4-chloro-2-fluorophenyl)-5-cyclohexyl-3-hydroxy-1,5-dihydro-2H-pyrrol-2-one)), was custom-labeled by Vitrax (Placentia, CA). [<sup>35</sup>S]GTPγS (guanosine 5'-*O*-(3-[<sup>35</sup>S]thio)triphosphate), with a specific activity of 1250 Ci mmol<sup>-1</sup>, was purchased from PerkinElmer (Waltham, MA). CCR2-RA-[R], SD-24 and JNJ-27141491 were synthesized as described previously.<sup>30, 37, 54</sup> BX471 was purchased from Cayman Chemical (Ann Arbor, MI, USA). Chemokine ligands CCL2 and CCL3 were purchased from PeproTech (Rocky Hill, NJ). Bovine serum albumin (BSA, fraction V) was purchased from Sigma (St. Louis, MO, USA). Bicinchoninic acid (BCA) and BCA protein assay reagent were purchased from Pierce Chemical Company (Rockford, IL, USA). Tango™ CCR1-*bla* and Tango™ CCR2-*bla* osteosarcoma (U2OS) cells stably expressing the human CCR1 or human CCR2b (U2OS-CCR1 or U2OS-CCR2, respectively) were obtained from Invitrogen (Carlsbad, CA). All other chemicals were obtained from standard commercial sources.

### Cell culture and membrane preparation

U2OS-CCR1 and U2OS-CCR2 were grown in a humidified atmosphere at 37 °C and 5% CO<sub>2</sub> in McCoy's 5A medium supplemented with 10% fetal calf serum, 2 mM glutamine, 0.1 mM nonessential amino acids (NEAAs), 25 mM HEPES, 1 mM sodium pyruvate, 100 IU/ml penicillin, 100 µg/ml streptomycin, 100 µg/ml G418, 50 µg/ml hygromycin, and 125 µg/ml zeocin (200 µg/ml zeocin for U2OS-CCR1). Cells were subcultured twice a week at a ratio of 1:3 to 1:8 on 10-cm Ø plates by trypsinization. For membrane preparation cells were subcultured on 15-cm Ø plates using dialyzed fetal calf serum. Membranes from U2OS-CCR1 and U2OS-CCR2 cells were prepared as described previously.<sup>26</sup> Briefly, cells were detached from confluent 15-cm Ø plates by scraping them into 5 ml of phosphate-buffered saline (PBS), collected and centrifuged for 5 minutes at 3000 rpm (700g). The pellets were resuspended in ice-cold 50 mM Tris-HCl buffer, pH 7.4, supplemented with 5 mM MgCl<sub>2</sub>, and homogenized with an Ultra Turrax homogenizer (IKA-Werke GmbH & Co. KG, Staufen, Germany). Membranes were separated from the cytosolic fraction by several centrifugation steps in an Optima LE-80 K ultracentrifuge (Beckman Coulter, Inc., Fullerton, CA) at 31,000 rpm for 20 minutes at 4°C. Finally, the membrane pellets were resuspended in 50 mM Tris-HCl buffer supplemented with 5 mM MgCl<sub>2</sub>, pH 7.4, divided into aliquots of 100 µl and 250 µl and stored at -80°C. Membrane protein concentrations were measured using a BCA protein determination with BSA as a standard.<sup>55</sup>

## **[<sup>3</sup>H]-CCR2-RA-[R] binding assays**

[<sup>3</sup>H]-CCR2-RA-[R] (homologous) displacement assays in U2OS-CCR1 and U2OS-CCR2 were performed in a 100  $\mu$ L reaction volume containing assay buffer (50 mM Tris-HCl, 5 mM MgCl<sub>2</sub> and 0.1% CHAPS, pH 7.4), 6 nM [<sup>3</sup>H]-CCR2-RA-[R], 8 to 15  $\mu$ g of membrane protein and the competing ligand. Homologous displacement assays were carried out with 3 different concentrations of [<sup>3</sup>H]-CCR2-RA-[R], namely 3, 6 and 12 nM. In all cases, at least 6 concentrations of competing ligand were used and the reaction mixture was incubated for 120 min at 25  $^{\circ}$ C. Non-specific binding was determined in the presence of 10  $\mu$ M CCR2-RA-[R]. Total radioligand binding did not exceed 10% of the amount added to prevent ligand depletion. [<sup>3</sup>H]-CCR2-RA-[R] saturation binding assays in U2OS-CCR2 were also performed in a 100  $\mu$ L reaction volume containing assay buffer, [<sup>3</sup>H]-CCR2-RA-[R] in 12 different concentrations ranging from 0.05 nM to 70 nM, and 15  $\mu$ g of membrane protein. Non-specific binding was determined in the presence of 10  $\mu$ M JNJ-27141491 at 4 different concentrations of radioligand, namely 0.1, 0.4, 2.5 and 20 nM. In association assays, U2OS-CCR1 and U2OS-CCR2 membrane preparations were added to the reaction mix at different time points of incubation, ranging from 1 min to 180 min incubation; in dissociation assays, membranes were first incubated with 6 nM [<sup>3</sup>H]-CCR2-RA-[R] for 90 min, and dissociation was initiated by the addition of 10  $\mu$ M CCR2-RA-[R] at different time points, up to 150 min for CCR1 and 180 min for CCR2. For all experiments, incubations were terminated by dilution with ice-cold wash-buffer (50 mM Tris-HCl buffer supplemented with 5mM MgCl<sub>2</sub> and 0.05% CHAPS, pH 7.4). Separation of bound from free radioligand was performed by rapid filtration through a 96-well GF/B filter plate using a Perkin Elmer Filtermate harvester (Perkin Elmer, Groningen, the Netherlands). Filters were washed 10 times with ice-cold wash buffer. 25  $\mu$ L of Microscint scintillation cocktail (Perkin-Elmer, Groningen, the Netherlands) was added to each well and the filter-bound radioactivity was determined by scintillation spectrometry using the P-E 2450 Microbeta<sup>2</sup> scintillation plate-counter (Perkin Elmer, Groningen, The Netherlands).

## **[<sup>35</sup>S]GTP $\gamma$ S Binding assays**

[<sup>35</sup>S]GTP $\gamma$ S binding assays were performed as described previously.<sup>26</sup> Briefly, binding assays were performed in a 100  $\mu$ L reaction volume containing assay buffer (50mM Tris-HCl, 5mM MgCl<sub>2</sub>, 100mM NaCl, 1mM EDTA, and 0.05% BSA, pH 7.4), 10  $\mu$ M GDP, 10  $\mu$ g of saponin and 10  $\mu$ g of membrane, either U2OS-CCR1 or U2OS-CCR2. To determine the EC<sub>50</sub> value of CCL2 and CCL3, the membrane mixture was preincubated with increasing concentrations of chemokine for 30 min at 25  $^{\circ}$ C. To determine the IC<sub>50</sub> values of the ligands, the membrane mixture was preincubated with increasing concentrations of the ligand of interest in absence



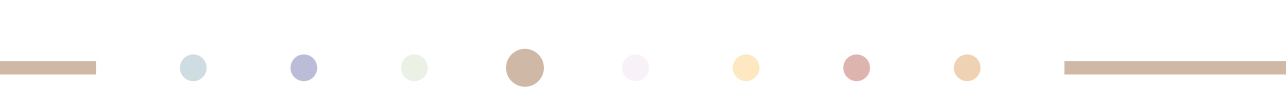
or presence of a fixed concentration of CCL2 (20 nM) or CCL3 (8 nM). Basal activity was determined in the absence of any ligand or chemokine. Finally, the mixture was incubated for another 90 min at 25 °C after the addition of 0.3 nM [<sup>35</sup>S]GTPγS in all cases. For all experiments, incubations were terminated by dilution with ice-cold 50mM Tris-HCl, 5mM MgCl<sub>2</sub> buffer. Separation of bound from free [<sup>35</sup>S]GTPγS was performed as described under “[<sup>3</sup>H]-CCR2-RA-[R] binding assays”.

## Data analysis

All experiments were analyzed using GraphPad Prism 7.0 (GraphPad Software Inc., San Diego, CA, U.S.A.). The  $K_D$  and  $B_{max}$  values of [<sup>3</sup>H]-CCR2-RA-[R] in U2OS-CCR2 were calculated from saturation experiments, by fitting the data to the equation  $Bound = (B_{max} * [L]) / ([L] + K_D)$ , where  $B_{max}$  is the maximum number of binding sites and  $K_D$  is the concentration required to reach half-maximum binding at equilibrium conditions. In the case of U2OS-CCR1 membranes, the  $K_D$  and  $B_{max}$  values were calculated from homologous binding experiments by non-linear regression analysis, using the “One site – Homologous” model that assumes that unlabeled and labeled CCR2-RA-[R] have identical affinities. The (p)IC<sub>50</sub> values of unlabeled ligands from [<sup>3</sup>H]-CCR2-RA-[R] binding assays were obtained by non-linear regression analysis of the displacement curves, and further converted into (p)K<sub>i</sub> values using the Cheng-Prusoff equation.<sup>56</sup> The (p)IC<sub>50</sub> or (p)EC<sub>50</sub> values from [<sup>35</sup>S]GTPγS curves were also obtained by non-linear regression. The observed association rate constants ( $k_{obs,fast}$ ;  $k_{obs,slow}$ ) were calculated by fitting the data to a two-phase exponential association function; similarly, dissociation rate constants ( $k_{off,fast}$ ;  $k_{off,slow}$ ) were calculated using a two-phase exponential decay function. All values obtained are means ± standard error of the mean (SEM) of at least three independent experiments performed in duplicate, unless stated otherwise. Differences in kinetic rates and pIC<sub>50</sub> values between receptors or between assay formats (in absence or presence of chemokine) were analyzed using an unpaired, two-tailed Student’s *t*-test with Welch’s correction; differences in pK<sub>i</sub> values between compounds, in maximal [<sup>35</sup>S]GTPγS inhibition against basal activity or in pseudo-Hill slopes from [<sup>35</sup>S]GTPγS inhibition curves against compound **45**, which showed a pseudo-Hill slope of approx. unity, were analyzed using a one-way ANOVA with Dunnett’s post-hoc test. Significant differences are displayed as \*,  $p < 0.05$ ; \*\*,  $p < 0.01$ ; \*\*\*,  $p < 0.001$ ; and \*\*\*\*,  $p < 0.0001$ .

## Computational Receptor Modeling and Docking

All modeling was performed in the Schrodinger suite,<sup>57</sup> Figures 3b and 3c were made in a later version<sup>58</sup> that includes the interaction and orientation of residues (e.g. backbone,



sidechain). As a starting point for the structure-based studies we used the recently published crystal structure of CCR2b in complex with both BMS-681 and CCR2-RA-[R] (PDB ID: 5T1A, **Chapter 3**).<sup>24</sup> We replaced the sequence (CCR2b: sequence between L226<sup>5x62</sup> and R240<sup>6x32</sup>) of the M2 muscarinic acetylcholine receptor, close to the intracellular binding site, by the CCR2b sequence using homology modelling<sup>59-61</sup> and CCR5 as template (PDB ID: 4MBS).<sup>62</sup> A homology model of CCR1 was constructed on the basis of this CCR2b model. For both models the knowledge-based scoring function was used. For the ligand docked, the  $pK_a$  of the hydroxyl hydrogen was calculated to be 4.5 using Jaguar;<sup>63, 64</sup> therefore, the negatively charged protonation state was used. Compound CCR2-RA-[R] was docked in both models using Induced fit docking.<sup>65, 66</sup> Visualizations were created using PyMOL;<sup>67</sup> residues within 5Å of the ligand and facing the binding site are shown.

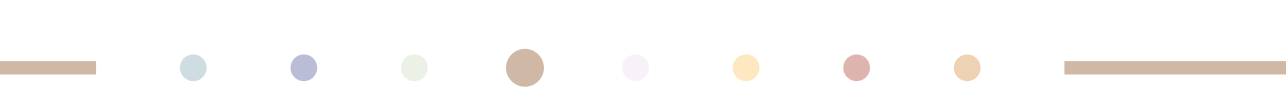


## REFERENCES

1. Griffith, J. W.; Sokol, C. L.; Luster, A. D. Chemokines and chemokine receptors: positioning cells for host defense and immunity. *Annu. Rev. Immunol.* **2014**, *32*, 659-702.
2. Bachelier, F.; Ben-Baruch, A.; Burkhardt, A. M.; Combadiere, C.; Farber, J. M.; Graham, G. J.; Horuk, R.; Sparre-Ulrich, A. H.; Locati, M.; Luster, A. D.; Mantovani, A.; Matsushima, K.; Murphy, P. M.; Nibbs, R.; Nomiyama, H.; Power, C. A.; Proudfoot, A. E.; Rosenkilde, M. M.; Rot, A.; Sozzani, S.; Thelen, M.; Yoshie, O.; Zlotnik, A. International union of basic and clinical pharmacology. LXXXIX. Update on the extended family of chemokine receptors and introducing a new nomenclature for atypical chemokine receptors. *Pharmacol. Rev.* **2014**, *66*, 1-79.
3. Kleist, A. B.; Getschman, A. E.; Ziarek, J. J.; Nevins, A. M.; Gauthier, P. A.; Chevigne, A.; Szpakowska, M.; Volkman, B. F. New paradigms in chemokine receptor signal transduction: moving beyond the two-site model. *Biochem. Pharmacol.* **2016**, *114*, 53-68.
4. Kufareva, I. Chemokines and their receptors: insights from molecular modeling and crystallography. *Curr. Opin. Pharmacol.* **2016**, *30*, 27-37.
5. Lopez-Cotarelo, P.; Gomez-Moreira, C.; Criado-Garcia, O.; Sanchez, L.; Rodriguez-Fernandez, J. L. Beyond chemoattraction: multifunctionality of chemokine receptors in leukocytes. *Trends Immunol* **2017**, *38*, 927 - 941.
6. Viola, A.; Luster, A. D. Chemokines and their receptors: drug targets in immunity and inflammation. *Annu Rev Pharmacol Toxicol.* **2008**, *48*, 171-197.
7. White, G. E.; Iqbal, A. J.; Greaves, D. R. CC chemokine receptors and chronic inflammation—therapeutic opportunities and pharmacological challenges. *Pharmacol. Rev.* **2013**, *65*, 47-89.
8. Pease, J.; Horuk, R. Chemokine receptor antagonists. *J. Med. Chem.* **2012**, *55*, 9363-9392.
9. Szekanecz, Z.; Koch, A. E. Successes and failures of chemokine-pathway targeting in rheumatoid arthritis. *Nat. Rev. Rheumatol.* **2016**, *12*, 5-13.
10. Haringman, J. J.; Smeets, T. J.; Reinders-Blankert, P.; Tak, P. P. Chemokine and chemokine receptor expression in paired peripheral blood mononuclear cells and synovial tissue of patients with rheumatoid arthritis, osteoarthritis, and reactive arthritis. *Ann. Rheum. Dis.* **2006**, *65*, 294-300.
11. Eltayeb, S.; Berg, A.-L.; Lassmann, H.; Wallström, E.; Nilsson, M.; Olsson, T.; Ericsson-Dahlstrand, A.; Sunnemark, D. Temporal expression and cellular origin of CC chemokine receptors CCR1, CCR2 and CCR5 in the central nervous system: insight into mechanisms of MOG-induced EAE. *J. Neuroinflammation* **2007**, *4*, 14.
12. Fife, B. T.; Huffnagle, G. B.; Kuziel, W. A.; Karpus, W. J. CC chemokine receptor 2 is critical for induction of experimental autoimmune encephalomyelitis. *J Exp Med* **2000**, 192.
13. Rottman, J. B.; Slavin, A. J.; Silva, R.; Weiner, H. L.; Gerard, C. G.; Hancock, W. W. Leukocyte recruitment during onset of experimental allergic encephalomyelitis is CCR1 dependent. *Eur. J. Immunol.* **2000**, *30*, 2372-2377.
14. Brühl, H.; Cihak, J.; Schneider, M. A.; Plachý, J.; Rupp, T.; Wenzel, I.; Shakarami, M.; Milz, S.; Ellwart, J. W.; Stangassinger, M.; Schlöndorff, D.; Mack, M. Dual role of CCR2 during initiation and progression of collagen-induced arthritis: evidence for regulatory activity of CCR2<sup>+</sup> T cells. *J. Immunol.* **2004**, *172*, 890-898.
15. Amat, M.; Benjamim, C. F.; Williams, L. M.; Prats, N.; Terricabras, E.; Beleta, J.; Kunkel, S. L.; Godessart, N. Pharmacological blockade of CCR1 ameliorates murine arthritis and alters cytokine networks in vivo. *Br. J. Pharmacol.* **2006**, *149*, 666-675.
16. Wang, Y.; Cui, L.; Gonsiorek, W.; Min, S.-H.; Anilkumar, G.; Rosenblum, S.; Kozlowski, J.; Lundell, D.; Fine, J. S.; Grant, E. P. CCR2 and CXCR4 regulate peripheral blood monocyte pharmacodynamics and link to efficacy in experimental autoimmune encephalomyelitis. *J. Inflamm.* **2009**, *6*, 32.

17. Dairaghi, D. J.; Zhang, P.; Wang, Y.; Seitz, L. C.; Johnson, D. A.; Miao, S.; Ertl, L. S.; Zeng, Y.; Powers, J. P.; Pennell, A. M.; Bekker, P.; Schall, T. J.; Jaen, J. C. Pharmacokinetic and pharmacodynamic evaluation of the novel CCR1 antagonist CCX354 in healthy human subjects: implications for selection of clinical dose. *Clin. Pharmacol. Ther.* **2011**, *89*, 726-734.
18. Tak, P. P.; Balanescu, A.; Tseluyko, V.; Bojin, S.; Drescher, E.; Dairaghi, D.; Miao, S.; Marchesin, V.; Jaen, J.; Schall, T. J. Chemokine receptor CCR1 antagonist CCX354-C treatment for rheumatoid arthritis: CARAT-2, a randomised, placebo controlled clinical trial. *Ann. Rheum. Dis.* **2013**, *72*, 337-344.
19. Horuk, R. Promiscuous drugs as therapeutics for chemokine receptors. *Expert Rev. Mol. Med.* **2009**, *11*, e1.
20. Sabroe, I.; Peck, M. J.; Van Keulen, B. J.; Jorritsma, A.; Simmons, G.; Clapham, P. R.; Williams, T. J.; Pease, J. E. A small molecule antagonist of chemokine receptors CCR1 and CCR3. Potent inhibition of eosinophil function and CCR3-mediated HIV-1 entry. *J. Biol. Chem.* **2000**, *275*, 25985-25992.
21. Junker, A.; Kokornaczyk, A. K.; Zweemer, A. J.; Frehland, B.; Schepmann, D.; Yamaguchi, J.; Itami, K.; Faust, A.; Hermann, S.; Wagner, S.; Schafers, M.; Koch, M.; Weiss, C.; Heitman, L. H.; Kopka, K.; Wunsch, B. Synthesis, binding affinity and structure-activity relationships of novel, selective and dual targeting CCR2 and CCR5 receptor antagonists. *Org. Biomol. Chem.* **2015**, *13*, 2407-2422.
22. Cox, B. D.; Prosser, A. R.; Sun, Y.; Li, Z.; Lee, S.; Huang, M. B.; Bond, V. C.; Snyder, J. P.; Krystal, M.; Wilson, L. J.; Liotta, D. C. Pyrazolo-piperidines exhibit dual inhibition of CCR5/CXCR4 HIV entry and reverse transcriptase. *ACS Med. Chem. Lett.* **2015**, *6*, 753-757.
23. Moriconi, A.; Cesta, M. C.; Cervellera, M. N.; Aramini, A.; Coniglio, S.; Colagioia, S.; Beccari, A. R.; Bizzarri, C.; Cavicchia, M. R.; Locati, M. Design of noncompetitive interleukin-8 inhibitors acting on CXCR1 and CXCR2. *J. Med. Chem.* **2007**, *50*, 3984-4002.
24. Zheng, Y.; Qin, L.; Ortiz Zacarias, N. V.; de Vries, H.; Han, G. W.; Gustavsson, M.; Dabros, M.; Zhao, C.; Cherney, R. J.; Carter, P.; Stamos, D.; Abagyan, R.; Cherezov, V.; Stevens, R. C.; Ilzerman, A. P.; Heitman, L. H.; Tebben, A.; Kufareva, I.; Handel, T. M. Structure of CC chemokine receptor 2 with orthosteric and allosteric antagonists. *Nature* **2016**, *540*, 458-461.
25. Oswald, C.; Rappas, M.; Kean, J.; Dore, A. S.; Errey, J. C.; Bennett, K.; Deflorian, F.; Christopher, J. A.; Jazayeri, A.; Mason, J. S.; Congreve, M.; Cooke, R. M.; Marshall, F. H. Intracellular allosteric antagonism of the CCR9 receptor. *Nature* **2016**, *540*, 462-465.
26. Zweemer, A. J.; Nederpelt, I.; Vrieling, H.; Hafith, S.; Doornbos, M. L.; de Vries, H.; Abt, J.; Gross, R.; Stamos, D.; Saunders, J.; Smit, M. J.; Ilzerman, A. P.; Heitman, L. H. Multiple binding sites for small-molecule antagonists at the CC chemokine receptor 2. *Mol. Pharmacol.* **2013**, *84*, 551-561.
27. Ortiz Zacarias, N. V.; Lenselink, E. B.; Ilzerman, A. P.; Handel, T. M.; Heitman, L. H. Intracellular receptor modulation: novel approach to target GPCRs. *Trends Pharmacol Sci* **2018**, *39*, 547-559.
28. Zweemer, A. J.; Bunnik, J.; Veenhuizen, M.; Miraglia, F.; Lenselink, E. B.; Vilums, M.; de Vries, H.; Gibert, A.; Thiele, S.; Rosenkilde, M. M.; Ilzerman, A. P.; Heitman, L. H. Discovery and mapping of an intracellular antagonist binding site at the chemokine receptor CCR2. *Mol. Pharmacol.* **2014**, *86*, 358-368.
29. Dasse, O.; Evans, J.; Zhai, H.-X.; Zou, D.; Kintigh, J.; Chan, F.; Hamilton, K.; Hill, E.; Eckman, J.; Higgins, P. Novel, acidic CCR2 receptor antagonists: lead optimization. *Letts. Drug. Des. Discov.* **2007**, *4*, 263-271.
30. Peace, S.; Philp, J.; Brooks, C.; Piercy, V.; Moores, K.; Smethurst, C.; Watson, S.; Gaines, S.; Zippoli, M.; Mookherjee, C.; Ife, R. Identification of a sulfonamide series of CCR2 antagonists. *Bioorg. Med. Chem. Lett.* **2010**, *20*, 3961-3964.
31. Buntinx, M.; Hermans, B.; Goossens, J.; Moechars, D.; Gilissen, R. A.; Doyon, J.; Boeckx, S.; Coesemans, E.; Van Lommen, G.; Van Wauwe, J. P. Pharmacological profile of JNJ-27141491 [(S)-3-[3, 4-difluorophenyl]-propyl]-5-isoxazol-5-yl-2-thioxo-2, 3-dihydro-1H-imidazole-4-carboxyl acid methyl ester], as a noncompetitive and orally active antagonist of the human chemokine receptor CCR2. *J. Pharmacol. Exp. Ther.* **2008**, *327*, 1-9.
32. Zou, D.; Dasse, O.; Evans, J.; Higgins, P.; Kintigh, J.; Kondru, R.; Schwartz, E.; Knerr, L.; Zhai, H. X. Pyrrolidinone Derivatives. U.S. Patent 6,727,275 B2. **2004**.
33. Zou, D.; Dasse, O.; Evans, J.; Higgins, P.; Kintigh, J.; Kondru, R.; Schwartz, E.; Knerr, L.; Zhai, H. X. Pyrrolidinone Derivatives. U.S. Patent Application 2003/0149081 A1. **2003**.

34. Kopp, M.; Lancelot, J. C.; Dallemagne, P.; Rault, S. Synthesis of novel pyrazolopyrrolopyrazines, potential analogs of sildenafil. *J. Heterocycl. Chem.* **2001**, *38*, 1045-1050.
35. Liang, M.; Mallari, C.; Rosser, M.; Ng, H. P.; May, K.; Monahan, S.; Bauman, J. G.; Islam, I.; Ghannam, A.; Buckman, B.; Shaw, K.; Wei, G. P.; Xu, W.; Zhao, Z.; Ho, E.; Shen, J.; Oanh, H.; Subramanyam, B.; Vergona, R.; Taub, D.; Dunning, L.; Harvey, S.; Snider, R. M.; Hesselgesser, J.; Morrissey, M. M.; Perez, H. D. Identification and characterization of a potent, selective, and orally active antagonist of the CC chemokine receptor-1. *J. Biol. Chem.* **2000**, *275*, 19000-19008.
36. Isberg, V.; de Graaf, C.; Bortolato, A.; Cherezov, V.; Katritch, V.; Marshall, F. H.; Mordalski, S.; Pin, J.-P.; Stevens, R. C.; Vriend, G.; Gloriam, D. E. Generic GPCR residue numbers – aligning topology maps while minding the gaps. *Trends Pharmacol. Sci.* **2015**, *36*, 22-31.
37. Zou, D.; Zhai, H.-X.; Eckman, J.; Higgins, P.; Gillard, M.; Knerr, L.; Carre, S.; Pasau, P.; Collart, P.; Grassi, J. Novel, acidic CCR2 receptor antagonists: from hit to lead. *Letts. Drug. Des. Discov.* **2007**, *4*, 185-191.
38. Kettle, J. G.; Faull, A. W.; Barker, A. J.; Davies, D. H.; Stone, M. A. N-benzylindole-2-carboxylic acids: potent functional antagonists of the CCR2b chemokine receptor. *Bioorg. Med. Chem. Lett.* **2004**, *14*, 405-408.
39. Cavallo, G.; Metrangolo, P.; Milani, R.; Pilati, T.; Priimagi, A.; Resnati, G.; Terraneo, G. The halogen bond. *Chem. Rev.* **2016**, *116*, 2478-2601.
40. Hansch, C.; Leo, A.; Taft, R. A survey of Hammett substituent constants and resonance and field parameters. *Chem. Rev.* **1991**, *91*, 165-195.
41. Chou, C. C.; Fine, J. S.; Pugliese-Sivo, C.; Gonsiorek, W.; Davies, L.; Deno, G.; Petro, M.; Schwarz, M.; Zavodny, P. J.; Hipkin, R. W. Pharmacological characterization of the chemokine receptor, hCCR1 in a stable transfectant and differentiated HL-60 cells: antagonism of hCCR1 activation by MIP-1 $\beta$ . *Br. J. Pharmacol.* **2002**, *137*, 663-675.
42. Gilliland, C. T.; Salanga, C. L.; Kawamura, T.; Trejo, J.; Handel, T. M. The chemokine receptor CCR1 is constitutively active, which leads to G protein-independent,  $\beta$ -arrestin-mediated internalization. *J. Biol. Chem.* **2013**, *288*, 32194-32210.
43. Prinz, H. Hill coefficients, dose-response curves and allosteric mechanisms. *J. Chem. Biol.* **2010**, *3*, 37-44.
44. Alvarez Arias, D.; Navenot, J.-M.; Zhang, W.-b.; Broach, J.; Peiper, S. C. Constitutive activation of CCR5 and CCR2 induced by conformational changes in the conserved TXP motif in transmembrane helix 2. *J. Biol. Chem.* **2003**, *278*, 36513-36521.
45. Lagorce, D.; Sperandio, O.; Baell, J. B.; Miteva, M. A.; Villoutreix, B. O. FAF-Drugs3: a web server for compound property calculation and chemical library design. *Nucleic Acids Res.* **2015**, *43*, W200-W207.
46. Lagorce, D.; Douguet, D.; Miteva, M. A.; Villoutreix, B. O. Computational analysis of calculated physicochemical and ADMET properties of protein-protein interaction inhibitors. *Sci. Rep.* **2017**, *7*, 46277.
47. Baell, J. B.; Holloway, G. A. New substructure filters for removal of pan assay interference compounds (PAINS) from screening libraries and for their exclusion in bioassays. *J. Med. Chem.* **2010**, *53*, 2719-2740.
48. Cormier, M.; Chardon, A.; Blanchet, J.; Rouden, J.; Maddaluno, J.; De Paolis, M. An organocatalytic access to spiro[4.5]decanes and spiro[4.6]undecanes containing aminolactones and 3-aminopyrrolidines. *Synthesis* **2015**, *47*, 2549-2553.
49. Koz'minykh, V.; Igidov, N.; Zykova, S.; Kolla, V.; Shuklina, N.; Odegova, T. Synthesis and pharmacological activity of 3-hydroxy-1,5-diaryl-4-pivaloyl-2,5-dihydro-2-pyrrolones. *Pharm. Chem. J.* **2002**, *36*, 188-191.
50. Kraïem, J. B.; Amri, H. Concise synthesis of  $\alpha$ -(hydroxymethyl) alkyl and aryl vinyl ketones. *Synth. Commun.* **2013**, *43*, 110-117.
51. Frank, R.; Bahrenberg, G.; Christoph, T.; Schiene, K.; De, V. J.; Damann, N.; Frommann, S.; Lesch, B.; Lee, J.; Kim, Y. S. Substituted Aromatic Carboxamide and Urea Derivatives as Vanilloid Receptor Ligands. Patent WO 2010/127855 A1. **2010**.
52. Carpino, P. A.; Sanner, M. A. Cannabinoid Receptor Ligands and Uses Thereof. Patent WO 2007/020502 A2. **2007**.

- 
53. Chonan, T.; Tanaka, H.; Yamamoto, D.; Yashiro, M.; Oi, T.; Wakasugi, D.; Ohoka-Sugita, A.; Ito, F.; Koretsune, H.; Hiratate, A. Design and synthesis of disubstituted (4-piperidinyl)-piperazine derivatives as potent acetyl-CoA carboxylase inhibitors. *Bioorg. Med. Chem. Lett.* **2010**, *20*, 3965-3968.
  54. Doyon, J.; Coesemans, E.; Boeckx, S.; Buntinx, M.; Hermans, B.; Van Wauwe, J. P.; Gilissen, R. A.; De Groot, A. H.; Corens, D.; Van Lommen, G. Discovery of potent, orally bioavailable small-molecule inhibitors of the human CCR2 receptor. *ChemMedChem* **2008**, *3*, 660-669.
  55. Smith, P. K.; Krohn, R. I.; Hermanson, G. T.; Mallia, A. K.; Gartner, F. H.; Provenzano, M. D.; Fujimoto, E. K.; Goeke, N. M.; Olson, B. J.; Klenk, D. C. Measurement of protein using bicinchoninic acid. *Anal. Biochem.* **1985**, *150*, 76-85.
  56. Cheng, Y.; Prusoff, W. H. Relationship between the inhibition constant (K<sub>1</sub>) and the concentration of inhibitor which causes 50 per cent inhibition (I<sub>50</sub>) of an enzymatic reaction. *Biochem. Pharmacol.* **1973**, *22*, 3099-3108.
  57. *Maestro Release 2017-1*; Schrödinger, LLC, New York, 2017.
  58. *Maestro Release 2017-2*; Schrödinger, LLC, New York, 2017.
  59. *Prime Release 2017-1*; Schrödinger, LLC, New York, 2017.
  60. Jacobson, M. P.; Friesner, R. A.; Xiang, Z.; Honig, B. On the role of the crystal environment in determining protein side-chain conformations. *J. Mol. Biol.* **2002**, *320*, 597-608.
  61. Jacobson, M. P.; Pincus, D. L.; Rapp, C. S.; Day, T. J.; Honig, B.; Shaw, D. E.; Friesner, R. A. A hierarchical approach to all-atom protein loop prediction. *Proteins* **2004**, *55*, 351-367.
  62. Tan, Q.; Zhu, Y.; Li, J.; Chen, Z.; Han, G. W.; Kufareva, I.; Li, T.; Ma, L.; Fenalti, G.; Li, J. Structure of the CCR5 chemokine receptor–HIV entry inhibitor maraviroc complex. *Science* **2013**, *341*, 1387-1390.
  63. *Jaguar Release 2017-1*; Schrödinger, LLC, New York, 2017.
  64. Bochevarov, A. D.; Harder, E.; Hughes, T. F.; Greenwood, J. R.; Braden, D. A.; Philipp, D. M.; Rinaldo, D.; Halls, M. D.; Zhang, J.; Friesner, R. A. Jaguar: a high-performance quantum chemistry software program with strengths in life and materials sciences. *Int. J. Quantum Chem.* **2013**, *113*, 2110-2142.
  65. *Glide Release 2017-1; Schrödinger Suite Prime 2017-1 Induced Fit Docking protocol*; Schrödinger, LLC, New York, 2017.
  66. Sherman, W.; Day, T.; Jacobson, M. P.; Friesner, R. A.; Farid, R. Novel procedure for modeling ligand/receptor induced fit effects. *J. Med. Chem.* **2006**, *49*, 534-553.
  67. *The PyMOL Molecular Graphics System*, version 1.8; Schrödinger, LLC, New York, 2015.

## SUPPORTING INFORMATION

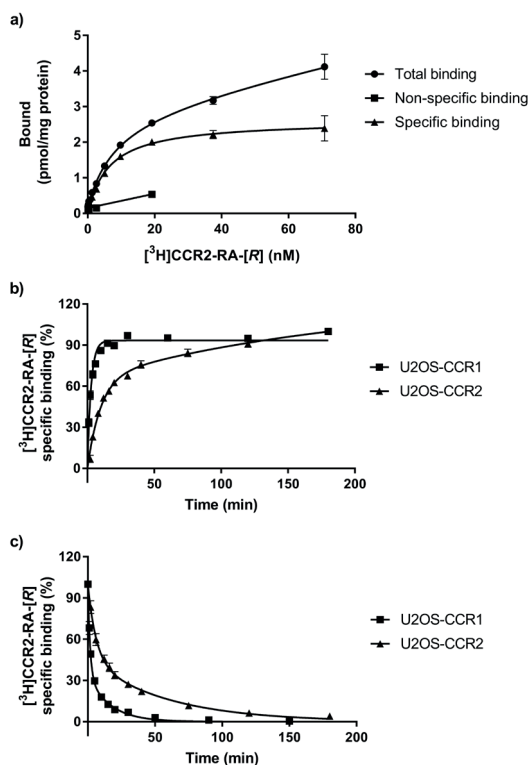


**Figure S1.** (a) Saturation binding of 0.05 – 70 nM  $[^3\text{H}]\text{-CCR2-RA-[R]}$  to U2OS-CCR2 at 25°C, in absence (total binding) or presence (non-specific binding) of 10  $\mu\text{M}$  JNJ-27141491. (b) Association kinetics of 6 nM  $[^3\text{H}]\text{-CCR2-RA-[R]}$  to U2OS-CCR1 (squares) and U2OS-CCR2 (triangles) at 25°C. In both CCR1 and CCR2, data were best fitted using a two-phase association function. (c) Dissociation kinetics of 6 nM  $[^3\text{H}]\text{-CCR2-RA-[R]}$  from U2OS-CCR1 (squares) and U2OS-CCR2 (triangles) at 25°C. In both CCR1 and CCR2, data were best fitted using a two-phase exponential decay function. For all experiments data shown are mean  $\pm$  SEM of at least three experiments performed in duplicate. See Supplementary Table 1 for  $pK_{D1}$ ,  $B_{max}$  and rate constants.

	TM1			TM2			TM3			TM6				TM7		H8						
B&W Number	1x53	1x56	1x57	2x39	2x40	2x43	3x46	3x50	3x53	6x30	6x32	6x33	6x34	6x36	6x37	6x40	7x53	7x56	8x47	8x48	8x49	8x50
hCCR2b	V	I	L	T	D	L	L	R	A	R	R	A	V	V	I	I	Y	V	G	E	K	F
hCCR1	V	V	L	T	S	L	L	R	A	K	K	A	V	L	I	I	Y	V	G	E	R	F

**Figure S2.** Sequence conservation of the key residues involved in the intracellular binding of CCR2-RA-[R] in CCR2,<sup>24</sup> as obtained by sequence alignment of human CCR1 and human CCR2b using the “Structure-based alignment” tool and the “Similarity search” tool of the GPCR database (GPCRdb, <http://www.gpcrdb.org>).<sup>36</sup> The residues are numbered according to the structure-based Ballesteros-Weinstein system,<sup>36</sup> which corresponds to the system used by the GPCRdb. Different amino acids in both CCR1 and CCR2 are highlighted.

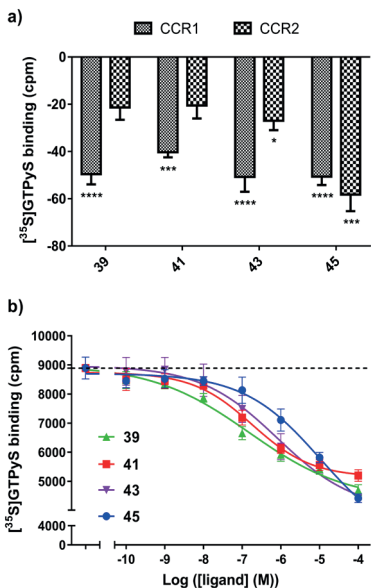


**Figure S3.** Compounds behave as inverse agonists in CCR1. (a) Maximal inhibition of CCL2 or CCL3-induced [<sup>35</sup>S]GTPyS binding achieved by the highest concentration tested of compounds **39**, **41**, **43** and **45** in U2OS-CCR1 (100 μM) and U2OS-CCR2 (**45** at 100 μM, **39**, **41**, **43** at 10 μM). One-way ANOVA with Dunnett's post-hoc test was performed to compare the maximal inhibition against basal [<sup>35</sup>S]GTPyS binding in CCR1 or CCR2. Significant differences are displayed as \*, *p* < 0.05; \*\*\*, *p* < 0.001; and \*\*\*\*, *p* < 0.0001. (b) Inhibition of basal [<sup>35</sup>S]GTPyS binding in absence of agonist CCL3 by compounds **39**, **41**, **43** and **45** in U2OS-CCR1. The level of basal activity in U2OS-CCR1 is indicated by a dashed line. Data shown are mean ± SEM of at least three experiments performed in duplicate.

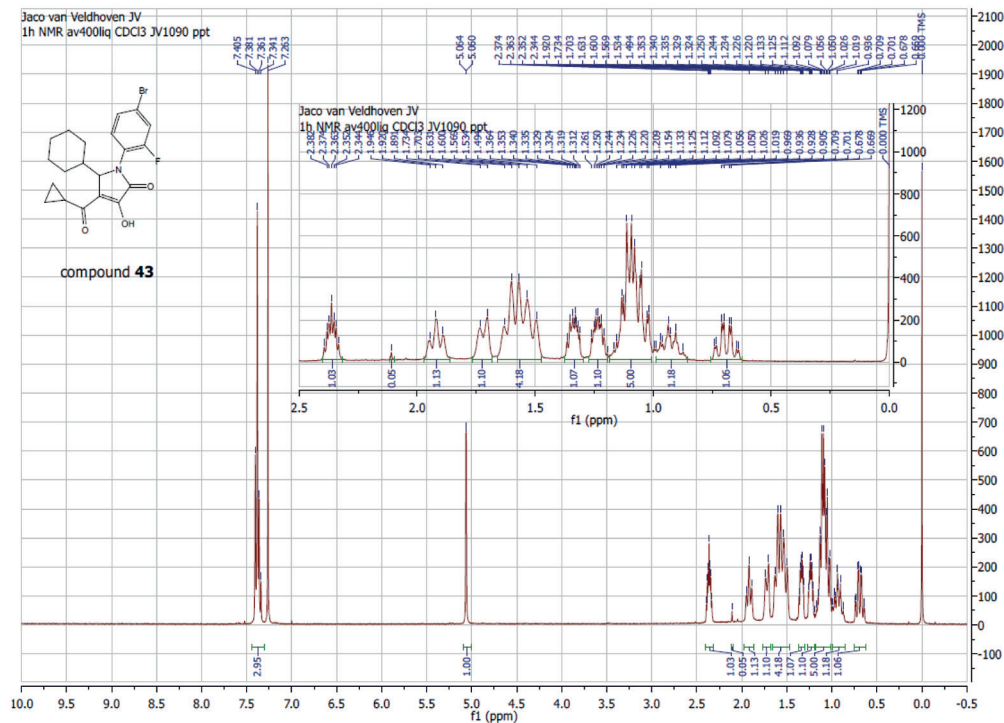


**Figure S4.** <sup>1</sup>H NMR spectrum of compound **43**, as an example of NMR interpretation.

**Table S1. Characterization of [<sup>3</sup>H]CCR2-RA-[R] in U2OS-CCR1 and U2OS-CCR2.<sup>a</sup>**

	U2OS-CCR1	U2OS-CCR2
$pK_D$ ( $K_D$ , nM)	7.87 ± 0.03 (13.5) <sup>b</sup>	8.20 ± 0.05 (6.3) <sup>c</sup>
$B_{max}$ (pmol/mg)	6.13 ± 0.24 <sup>b</sup>	2.63 ± 0.28 <sup>c</sup>
$k_{obs,fast}$ (min <sup>-1</sup> ) <sup>d</sup>	0.69 ± 0.08	0.12 ± 0.01*
$k_{obs,slow}$ (min <sup>-1</sup> ) <sup>d</sup>	0.11 ± 0.007	0.01 ± 0.001**
%fast	62 ± 2	55 ± 3
$k_{off,fast}$ (min <sup>-1</sup> ) <sup>e</sup>	0.62 ± 0.08	0.18 ± 0.02*
$k_{off,slow}$ (min <sup>-1</sup> ) <sup>e</sup>	0.06 ± 0.002	0.02 ± 0.002***
%fast	66 ± 2	54 ± 4

<sup>a</sup>Values are means ± SEM of at least three independent experiments performed in duplicate. Unpaired *t*-test analysis with Welch's correction was performed to analyze differences in kinetic rates between receptors, with differences noted as \*, *p* < 0.05; \*\*, *p* < 0.01; \*\*\*, *p* < 0.001. <sup>b</sup>Values obtained from homologous displacement of 3, 6 and 12 nM [<sup>3</sup>H]-CCR2-RA-[R] from U2OS-CCR1 at 25°C. <sup>c</sup>Values obtained from saturation binding of 0.05 – 70 nM [<sup>3</sup>H]-CCR2-RA-[R] to U2OS-CCR2 at 25°C. <sup>d</sup>Observed association and <sup>e</sup>dissociation rate constants of [<sup>3</sup>H]-CCR2-RA-[R] in U2OS-CCR1 or -CCR2 at 25°C.

**Table S2. Inhibition of basal [<sup>35</sup>S]GTPγS binding, i.e. in the absence of agonist CCL3, by compounds 37, 39, 41 and 43 in U2OS-CCR1.**

Compound	$pIC_{50} \pm SEM$ ( $IC_{50}$ , μM) <sup>a</sup>	Hill slope <sup>a</sup>
39	6.78 ± 0.04 (0.17)**	-0.4 ± 0.06*
41	6.70 ± 0.08 (0.21)**	-0.6 ± 0.05
43	6.13 ± 0.15 (0.85)	-0.4 ± 0.07*
45	5.17 ± 0.01 (6.73)	-0.5 ± 0.07*

<sup>a</sup>All values are means ± SEM of at least three independent experiments performed in duplicate. Unpaired *t*-test analysis with Welch's correction was performed to analyze differences in their inhibitory potencies and pseudo-Hill slopes as antagonists and inverse agonists in CCR1, with differences noted as \*, *p* < 0.05; and \*\*, *p* < 0.01.

